Class Notes, 31415 RF-Communication Circuits

Chapter II

RF-CIRCUITS

Jens Vidkjær

NB230

Contents

II RF-Circuits, Concepts and Methods

In RF-communication system, control of frequency bands and impedance matching conditions between functional blocks or amplifier stages are problems that constantly face a circuit designer. The tasks are so frequent that many analytical techniques and approximation methods especially suited for high-frequency circuits have evolved and strongly influenced the jargon of RF engineering. Below we shall introduce the most important basic concepts and methods that are required to

- understand data sheets and literature,
- make simpler design decisions or calculations, and
- prepare and interpret simulation data.

The selection of topics and examples have furthermore been conducted to suit the needs in the following chapters, which are still in preparation.

Scanning contents, the chapter starts summarizing basic properties of resonance circuits. Although significant by themselves, the importance of acquiring familiarity with ideal resonance circuits is the fact, that any narrowbanded resonance circuit may be approximated by the ideal ones around resonance frequencies. This property reduces significantly the efforts that are required to understand and explore operations of tuned bandpass circuits, which are frequently used in RF-communication systems. Foundations of the simplifications are dealt with in sections concerning narrowband approximations and series-to-parallel transformations. The tuned amplifiers are introduced in ideal form concentrating on simple frequency characteristics. Coupling techniques using transformers and coupled resonance circuits are still highly useful methods in RF-designs, so they are considered in some details here. Finally, the very general method of constructing lumped element matching networks using a Smith chart is exemplified.

Power matching is fundamental for designing and understanding many RF circuits. Although this concept is mandatory in basic circuit theory curriculums, it is repeated for convenience in an appendix. Also the method of illustrating and solving network equations by the signal flow graph method is summarized in an appendix.

II-1 Parallel Resonance Circuits

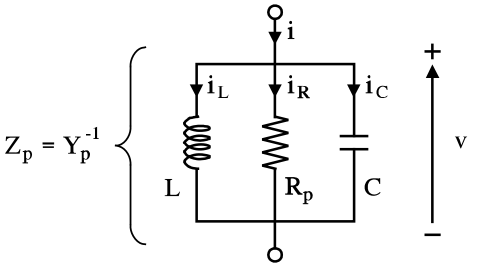

Fig.1 Parallel resonance circuit

$$\textit{resonance frequency}: \quad \omega_0 = \frac{1}{\sqrt{LC}}$$

$$\textit{quality factor}: \quad Q = \frac{R_p}{L\,\omega_0} = R_p C\,\omega_0 \qquad (1)$$

$$\textit{damping ratio}: \quad \zeta = \frac{1}{2R_p}\sqrt{\frac{L}{C}} = \frac{1}{2Q}$$

A basic parallel resonance circuit is shown in Fig.1. Besides component values the combinations, which are summarized by Eq.(1), are frequently used. The resonance frequency is the frequency where the capacitive and the inductive susceptances are equal in magnitude as indicated in Fig.2a. When an external steady state sinusoidal voltage-source of frequency ω_0 is applied to the resonance circuit, the two opposite currents through the capacitor and the inductor balance each other, and only the resistor current flows through the terminal. This situation is sketched in Fig.2b, which also shows how the quality factor Q indicates the magnitude ratio of the internal reactive currents over the resistive terminal current at resonance.

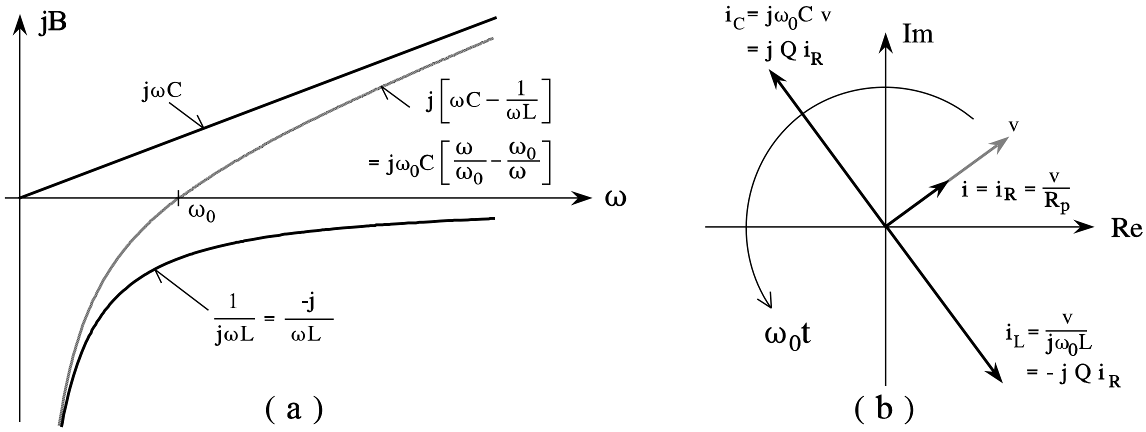

Fig.2 Parallel resonance. (a) Susceptance composition as function of frequency. (b) Current and voltage phasors at the resonance frequency ω_0.

Another view upon resonance and the quality factor concerns the energy in the circuit under steady state conditions. At instants where the two phasors i_C and i_L are perpendicular to the real axis, no currents flow into the capacitor or inductor, but the capacitor hold maximum energy

$$E_{Cmax} = \tfrac{1}{2}\, C\, V_{Cpeak}^2 = C\, v^2 \qquad (2)$$

The first equation is the usual electrostatic energy expression. The second takes into account that rms values - indicated by small letters - are conventionally used when dealing with steady state linear circuits. A quarter of a period later the current phasors project in full onto the real axis while the voltage is zero. The capacitor holds no energy, but the inductor energy peaks with the same maximum that formerly was held in the capacitor,

$$E_{Lmax} = \frac{1}{2} L\, I_{L,peak}^2 = L\, i_L^2 = L \frac{v^2}{\omega_0^2 L^2} = C\, v^2 = E_{Cmax} \tag{3}$$

Thus, a constant amount of energy laps between the capacitor and the inductor at resonance, and the quality factor may be expressed

$$Q = 2\pi \left. \frac{\textit{Energy kept in circuit}}{\textit{Energy loss per cycle}} \right|_{\omega=\omega_0} = 2\pi \frac{C v^2}{T_0 v^2 / R_p} = R_p C \omega_0 \,, \tag{4}$$

where the loss is calculated as the resistor power times the resonance period $T_0 = 2\pi/\omega_0$. This interpretation of resonance is often useful in the construction of lumped circuit equivalents for the variety of electromagnetic and mechanical resonators that are used in RF-circuits.

Frequency Response

Expressed through circuit element values, the impedance function for the parallel circuit in Fig.1 is

$$Z_p(s) = \frac{1}{Y_p(s)} = \frac{1}{sC + 1/sL + 1/R_p} = \frac{R_p}{1 + sCR_p + R_p/sL} \,. \tag{5}$$

Introducing ω_0 and Q from Eq.(1), the impedance expressed as a function of frequency $s=j\omega$ becomes

$$Z_p(j\omega) = \frac{R_p}{1 + jQ\,\beta(\omega)} \,, \qquad \textit{where} \quad \beta(\omega) = \left(\frac{\omega}{\omega_0} - \frac{\omega_0}{\omega} \right) . \tag{6}$$

The frequency dependency of the impedance is kept in the quantity $\beta(\omega)$, which is zero at the resonance frequency ω_0. Here the denominator of Eq.(6) gets its smallest size and the impedance has maximum R_p, the parallel resistance. The magnitude and phase of $Z_p(j\omega)$ are

$$\left| Z_p(j\omega) \right| = \frac{R_p}{\sqrt{1 + Q^2 \beta^2(\omega)}} \,, \qquad \angle Z_p(j\omega) = -\tan^{-1}\{ Q\,\beta(\omega) \} \,. \tag{7}$$

The two functions are shown in Fig.3(a) while Fig.3(b) shows the corresponding admittance characteristics,

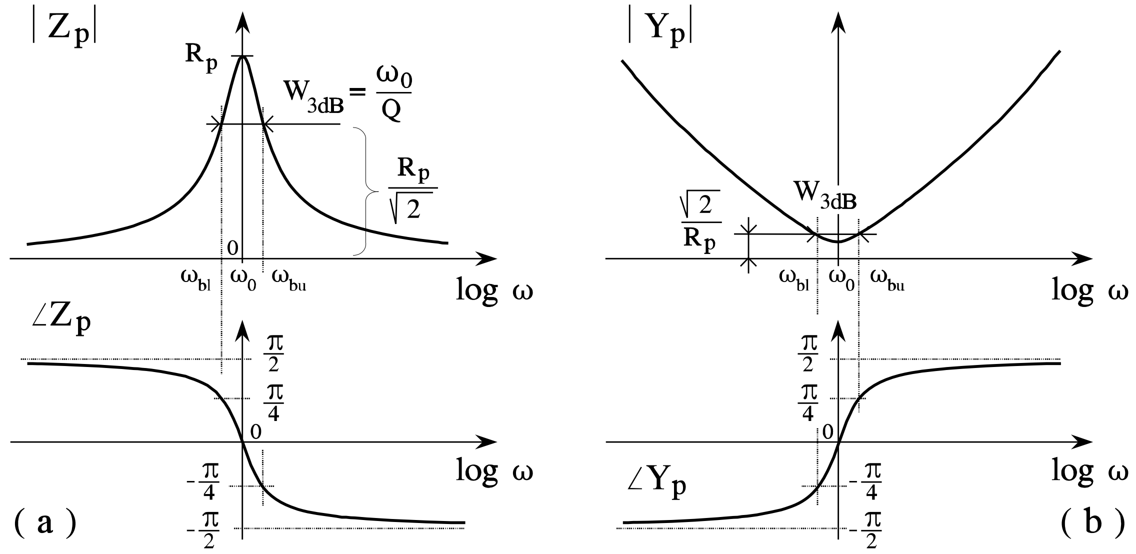

Fig.3 Impedance (a) and admittance (b) magnitudes and phases of the parallel resonance circuit in Fig.1. The curves are symmetric around ω_o due to the logarithmic frequency scales.

$$\left|Y_p(j\omega)\right| = \frac{1}{\left|Z_p(j\omega)\right|} = \frac{\sqrt{1+Q^2\beta^2(\omega)}}{R_p}, \qquad \angle Y_p(j\omega) = -\angle Z_p(j\omega) = \tan^{-1}\{Q\beta(\omega)\}. \tag{8}$$

Upper and lower bounds of the 3dB bandwidth intervals W_{3dB}, which are indicated in Fig.3 , correspond to a denominator size equal to $\sqrt{2}$ in Eq.(7). The bounds are found setting the imaginary part of the denominator equal in magnitude to the real part, i.e.

$$\begin{gathered} Q\beta(\omega_b) = \pm 1: \quad \frac{\omega_b}{\omega_0} - \frac{\omega_0}{\omega_b} = \pm\frac{1}{Q} \quad \Rightarrow \quad \omega_b^2 \pm \frac{\omega_0}{Q}\,\omega_b - \omega_0^2 = 0 \quad \Rightarrow \\ \omega_b = \pm\frac{\omega_0}{2Q} \pm \omega_0\sqrt{1+\frac{1}{4Q^2}} = \begin{cases} \pm\,\omega_{bu}\,, & \textit{upper 3dB bounds} \\ \pm\,\omega_{bl}\,, & \textit{lower 3dB bounds} \end{cases} \end{gathered} \tag{9}$$

Both negative and positive frequencies are contained in the conditions. We call the largest valued solutions, where the two terms in ω_b have equal signs, the upper bounds $\pm\omega_{bu}$. The lower bounds $\pm\omega_{bl}$ are obtained with terms of opposite signs. Fig.4 summarizes how the different solutions are formed. By definition, the 3dB bandwidth is taken to be the distance between positive or zero-valued 3dB frequency bounds, and we get the result that was incorporated in Fig.3,

$$W_{3dB} = \omega_{bu} - \omega_{bl} = \frac{\omega_0}{Q}\,. \tag{10}$$

It follows from the solutions in Eq.(9) that the resonance frequency ω_0 is not centered between the 3dB bounds but is the geometrical mean of the bounds,

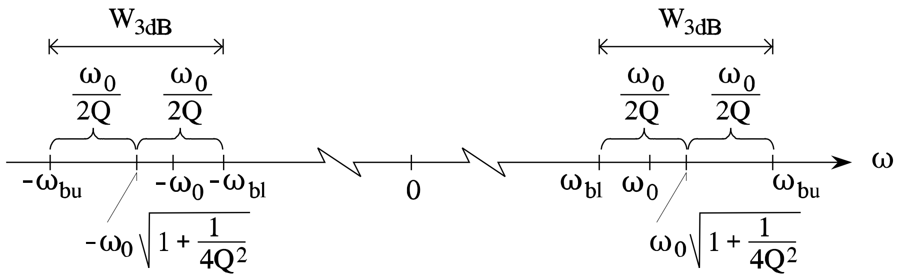

Fig.4 Upper and lower 3dB bound positions from Eq.(9) . Note, in linear frequency scale the 3dB bands are not symmetric around the resonances at $\pm\omega_0$ unless $Q \to \infty$.

$$\omega_{bu}\,\omega_{bl} = \omega_0^2\left(\frac{1}{2Q}+\sqrt{1+\frac{1}{4Q^2}}\right)\left(\frac{-1}{2Q}+\sqrt{1+\frac{1}{4Q^2}}\right) = \omega_0^2\,, \tag{11}$$

$$\frac{\omega_0}{\omega_{bl}} = \frac{\omega_{bu}}{\omega_0} \quad\Rightarrow\quad \log\omega_0 - \log\omega_{bl} = \log\omega_{bu} - \log\omega_0\,, \tag{12}$$

so in logarithmic frequency scale the upper and lower 3dB frequency bounds are symmetric with respect to $\log\omega_0$. However, any other pair of frequencies, ω_u,ω_l that has the resonance frequency as geometrical mean maps symmetrically around $\log\omega_0$. Since both frequencies provide the same absolute $|\beta|$, i.e.

$$\frac{\omega_0}{\omega_l} = \frac{\omega_u}{\omega_0} \quad\Rightarrow\quad \beta(\omega_u) = \frac{\omega_u}{\omega_0} - \frac{\omega_0}{\omega_u} = \frac{\omega_0}{\omega_l} - \frac{\omega_l}{\omega_0} = -\beta(\omega_l)\,, \tag{13}$$

the impedance or admittance magnitude characteristics of the types in Fig.3 have even symmetry with respect to the resonance frequency in a logarithmic frequency scale. Correspondingly, the phase characteristics show odd symmetry because $\tan^{-1}(-Q\beta)=-\tan^{-1}(Q\beta)$. At the 3dB boundaries where $|Q\beta|=1$, the phase angles of impedance Z_p become $\pm\frac{1}{4}\pi$. Fig.5 shows plots of the impedance function with various Q-factors. The normalization in magnitude corresponds to keeping the inductor and capacitor fixed while letting the parallel resistance follows Q according to Eq.(1). The asymptotic behavior of the impedance approximating the inductor reactance below and the capacitor reactance above resonance respectively are readily observed. Calculating magnitudes, it may suffice to use the inductor or capacitor alone at frequencies that differ more than a factor of three from resonance.

Summarizing the frequency characteristics, we have seen that the greater Q, the smaller bandwidth and in turn, the steeper phase characteristics around the resonance frequency ω_0. Moreover, the frequency characteristics were symmetric in logarithmic frequency scale. Phase steepness is an important property when a resonance circuit is employed in an oscillator and we shall return to this question later. Also, the symmetry property will be reconsidered. Important classes of signal handling expect linear symmetry that may be approached with high

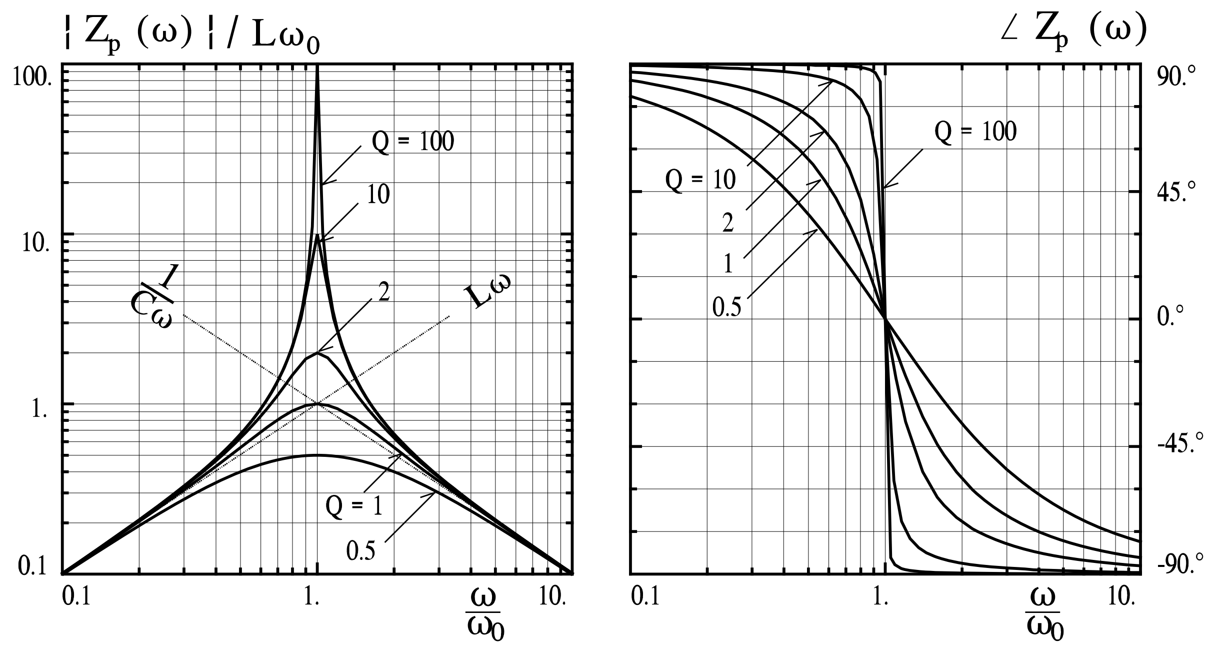

Fig.5 Normalized magnitudes and phases in the impedance of parallel tuned circuits with varying Q-factors.

Q circuits too.[1] For obvious reasons such circuits are also called narrowbanded.

Poles and Zeros

Pole and zero positions are useful for investigating responses of frequency selective networks that include parallel tuned circuits. Using parameters from Eq.(1), the impedance Z_p of Eq.(5) is rewritten,

$$Z_p(s) = \frac{s/C}{s^2 + s\,2\zeta\omega_0 + \omega_0^2} = \frac{s/C}{s^2 + s\omega_0/Q + \omega_0^2} \ . \tag{14}$$

Solving for the s-values, which set the numerator and the denominator equal to zero respectively, gives the zero and the poles of the impedance function. Once poles and zeros are known, the impedance may be cast in the form that suits the analysis of composite networks,

$$Z_p(s) = \frac{1}{C}\,\frac{(s - s_0)}{(s - s_1)(s - s_2)} \ . \tag{15}$$

1) See section VI-1 on frequency stability in oscillators and section I-4 on transmission of narrowband signals.

While there is a tradition of using Q for characterizing frequency responses of resonant RF circuits, the conceptually equivalent damping ratio ζ is often seen in pole-zero and especially transient response calculations, where it leads to more compact expressions. We proceed here with both forms and get,

$$zero\,|_{Z_p}: \quad s_0 = 0\,,$$
$$poles\,|_{Z_p}: \quad s_{1,2} = \omega_0 \left\{ -\zeta \pm \sqrt{\zeta^2 - 1} \right\} = \omega_0 \left\{ -\frac{1}{2Q} \pm \sqrt{\frac{1}{4Q^2} - 1} \right\}. \tag{16}$$

Up to this point no attention was given to actual parameter values. The last result requires a distinction between circuits having $\zeta \geq 1$ and $\zeta < 1$ ($Q \leq \frac{1}{2}$ and $Q > \frac{1}{2}$). In first case the square roots of Eq.(16) are real and the poles are on the real axis. In second case the poles move from the real axis and make a complex conjugated pair. To emphasize this property we change the last part of Eq.(16) to read

$$\begin{aligned} poles|_{Z_p}:\ s_{1,2} &= \omega_0 \left\{ -\zeta \pm j\sqrt{1-\zeta^2} \right\} = \omega_0 \left\{ -\frac{1}{2Q} \pm j\sqrt{1 - \frac{1}{4Q^2}} \right\}, & (a) \\ &\underset{\zeta<1}{\approx} \omega_0 \left\{ -\zeta \pm j\left[1 - \frac{\zeta^2}{2}\right] \right\} \underset{Q>1}{\approx} \omega_0 \left\{ -\frac{1}{2Q} \pm j\left[1 - \frac{1}{8Q^2}\right] \right\}, & (b) \\ &\underset{\zeta\ll 1}{\approx} -\zeta\,\omega_0 \pm j\,\omega_0 \qquad \underset{Q\gg 1}{\approx} -\frac{\omega_0}{2Q} \pm j\,\omega_0\,. & (c) \end{aligned} \tag{17}$$

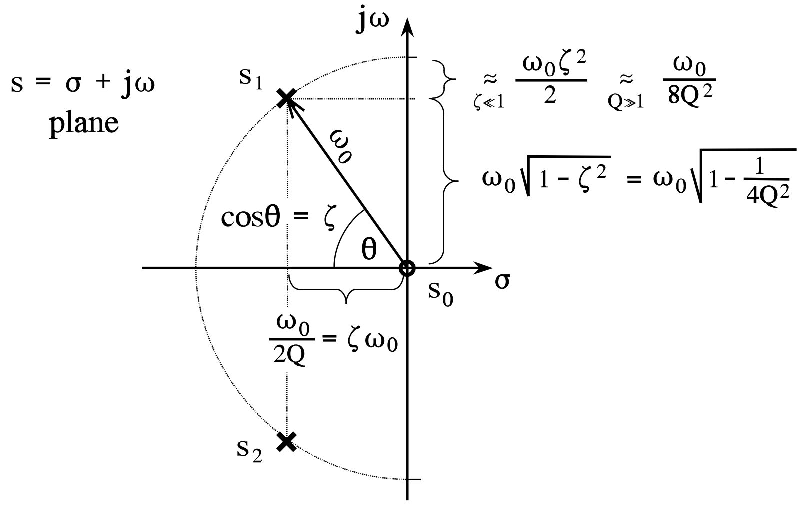

Fig.6 Position of poles s_1, s_2, and the zero s_0 in the impedance $Z_p(s)$ of the parallel resonance circuit with $\zeta<1$ or $Q>\frac{1}{2}$.

The square roots in (a) are real valued if the poles are complex. The approximations in the following lines apply to lightly damped circuits with higher and higher Q´s, where the expressions in Eq.(17)(b) are based on the estimate

$$\sqrt{1 + x} \approx 1 + \frac{1}{2} x \qquad for \qquad |x| \ll 1 \, . \tag{18}$$

Fig.6 sketches the geometry of complex pole and zero positions. Starting from damping ζ=1 (Q=½) the poles are by Eq.(17)(a) constrained to move along a circle of radius ω_0 from the real towards the imaginary axis with declining damping or growing Q. Once the poles and zeros are known, the frequency characteristics of Z_p may be calculated from geometrical considerations as sketched in Fig.7 and Eqs.(19) to (21).

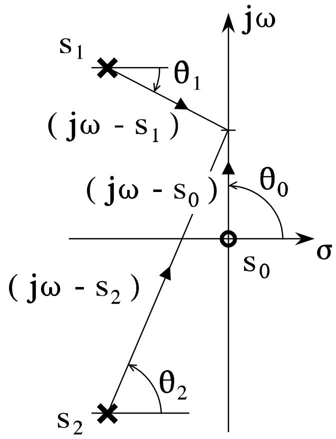

$$Z_p(j\omega) = \frac{(j\omega - s_0)}{C (j\omega - s_1)(j\omega - s_2)} \, , \tag{19}$$

$$\left| Z_p(j\omega) \right| = \frac{| j\omega - s_0 |}{C | j\omega - s_1 || j\omega - s_2 |} \, , \tag{20}$$

$$\angle Z_p(j\omega) = \theta_0 - \theta_1(j\omega) - \theta_2(j\omega). \tag{21}$$

Fig.7 Calculation of $Z_p(\omega)$ from poles and zeros

Transient Response

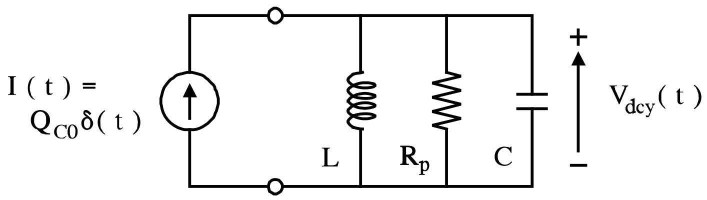

Fig.8 Charging of capacitor C to voltage $V_{C0} = Q_{C0}/C$.

The projection of the poles on the imaginary axis determines the oscillatory modes in the transient responses of the circuit. To see this, we consider the decay of circuit energy when the circuit is left alone once the capacitor has been charged to a voltage of V_{C0} with the inductor current initialized to zero. The initial charging of the capacitor is equivalent to forcing a pulse current of strength

$$I(t) = Q_{C0} \, \delta(t) = C \, V_{C0} \, \delta(t) \tag{22}$$

through the circuit as indicated by Fig.8.[2] The corresponding transient voltage decay $V_{dcy}(t)$ is the impulse response of the impedance function, which is given by its inverse Laplace transform, i.e.

$$\begin{aligned} V_{dcy}(t) &= V_{C0} C\, \mathcal{L}^{-1}\{ Z_p(s) \} = V_{C0}\, \mathcal{L}^{-1}\left\{ \frac{s}{s^2 + 2\zeta\omega_0 s + \omega_0^2} \right\} \\ &= V_{C0} \mathcal{L}^{-1}\left\{ \frac{[\, s + \zeta\omega_0 \,] - \zeta\omega_0}{[\, s+\zeta\omega_0 \,]^2 + \omega_0^2 [\, 1 - \zeta^2 \,]} \right\} . \end{aligned} \tag{23}$$

The last rewriting prepares for use of standard Laplace transform tables, from which we get

$$V_{dcy}(t) = V_{C0}\, e^{-\zeta\omega_0 t} \times \begin{cases} \cos\left(\sqrt{1-\zeta^2}\,\omega_0 t \right) - \dfrac{\zeta \sin\left(\sqrt{1-\zeta^2}\,\omega_0 t \right)}{\sqrt{1-\zeta^2}} , & \zeta < 1, \\ \left[\, 1 - \omega_0 t \,\right] , & \zeta = 1, \\ \cosh\left(\sqrt{\zeta^2 - 1}\,\omega_0 t \right) - \dfrac{\zeta \sinh\left(\sqrt{\zeta^2-1}\,\omega_0 t \right)}{\sqrt{\zeta^2-1}} , & \zeta > 1, \end{cases} \tag{24}$$

where the angular frequency is recognized as the size of the imaginary pole component if $\zeta<1$. Introducing the auxiliary phases and the identities

$$\phi_1 = \tan^{-1}\left(\zeta \,/\, \sqrt{1-\zeta^2} \right) , \qquad \phi_2 = \coth^{-1}\left(\zeta \,/\, \sqrt{\zeta^2 - 1} \right) , \tag{25}$$

$$\cos(a \pm b) = \cos a \, \cos b \mp \sin a \, \sin b , \tag{26}$$

$$\sinh(a \pm b) = \sinh a \, \cosh b \pm \cosh a \, \sinh b , \tag{27}$$

the time domain responses may be condensed to read

$$V_{dcy}(t) = V_{C0}\, e^{-\zeta\omega_0 t} \times \begin{cases} \dfrac{1}{\cos\phi_1} \cos\left(\sqrt{1-\zeta^2}\,\omega_0 t + \phi_1 \right) , & \zeta < 1, \\ \left[\, 1 - \omega_0 t \,\right] , & \zeta = 1, \\ \dfrac{1}{\sinh\phi_2} \sinh\left(\phi_2 - \sqrt{\zeta^2-1}\,\omega_0 t \right) , & \zeta > 1. \end{cases} \tag{28}$$

---

2) Note, the delta function $\delta(t)$ has dimension [sec^{-1}] to comply with the requirement $\int_{-\infty}^{\infty} \delta(t)\, dt = 1$.

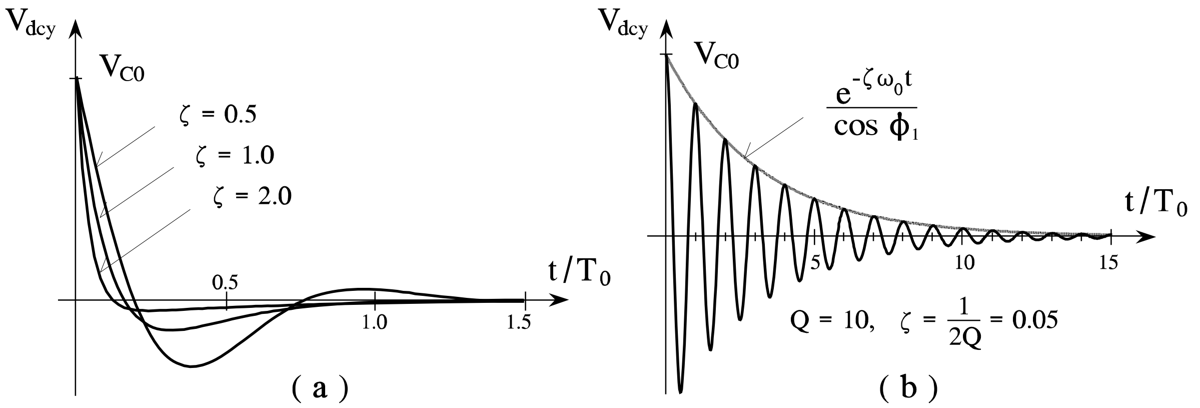

Fig.9 Transients from Eq.(28). Examples in (a) are heavily damped and (b) is lightly damped. Time scales are in units of the resonance period $T_0=2\pi/\omega_0$.

Fig.9 shows examples of the responses with different dampings. The case $\zeta=1$, where the two poles coincide on the real axis, sets the border between aperiodic and oscillatory solutions. In the latter case, the leading exponential factor shapes the envelope to the solution

$$envelope,\ \zeta < 1 : \qquad \frac{1}{\cos\phi_1}\, e^{-\zeta\omega_0 t} = \frac{1}{\cos\phi_1}\, e^{-t/\tau_{dcy}} . \tag{29}$$

The corresponding time constant,

$$\tau_{dcy} = \frac{1}{\zeta\,\omega_0} = \frac{2Q}{\omega_0} = 2R_pC , \tag{30}$$

is sometimes called the logarithmic decrement of the circuit. Observe that the result is in agreement with the previous equivalent baseband considerations in example I-4-2. In practical terms we notice that the significant number of cycles through the decay approximates Q if Q $>\approx 5$ so $\zeta \approx< 0.1$ and $\cos\phi_1 \approx 1$. It follows from the fact that at $t=QT_0$, the exponential has fallen from one to

$$e^{-QT_0/\tau_{dcy}} = e^{-\pi} = 0.0432 \qquad i.e. \qquad (e^{-\pi})^2 = 0.00186 , \tag{31}$$

so more than 99.8% of the initial energy is lost in the resistor at that instant.

II-2 Series Resonance Circuit Summary

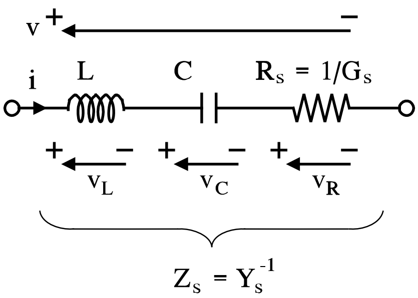

Fig.10 Series resonance circuit

$$\textit{resonance frequency}: \quad \omega_0 = \frac{1}{\sqrt{LC}}$$

$$\textit{quality factor}: \quad Q = \frac{L\omega_0}{R_s} = \frac{1}{R_s C \omega_0} \tag{32}$$

$$\textit{damping ratio}: \quad \zeta = \frac{R_s}{2}\sqrt{\frac{C}{L}} = \frac{1}{2Q}$$

A series resonance circuit is connected as shown by Fig.10 and Eq.(32) summarizes its common parameter combinations. The circuit admittance and impedance are,

$$Y_s(s) = \frac{1}{Z_s(s)} = \frac{1}{sL + 1/sC + R_s} \tag{33}$$

Compared to the parallel circuit impedance and admittance in Eq.(5) it is seen, that the numerator and denominator are similar in structure with respect to s, but the coefficients are different. Connected to a source, the two types of resonance circuits behave in duality. This means that the reader could kindly be asked to repeat the preceding section exchanging terms, voltage and current, parallel and series, impedance and admittance, inductance and capacitance, resistance and conductance, and then we were done. To avoid confusion in future references, however, the main concept of the series resonance is summarized below in its own terms, but without detailed derivations.

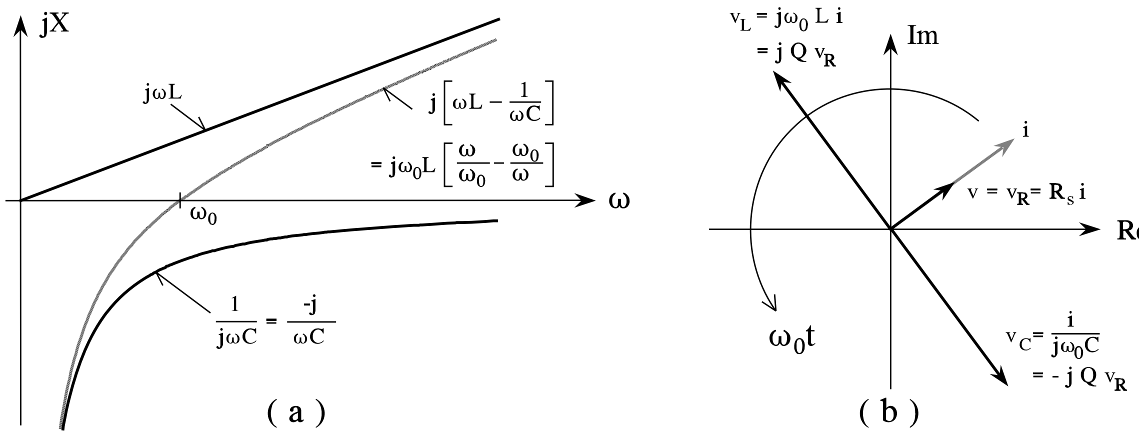

Fig.11 Series resonance. (a) Reactance composition as function of frequency. (b) Voltage and current phasors at the resonance frequency ω_0.

At resonance in a series circuit the voltages across the inductive and the capacitive reactances are equal in magnitudes but opposed in phases. With the same current flowing through all components the requirement is that the two reactances balance each other at the resonance frequency as indicated by Fig.11(a). The phasor diagram in Fig.11(b) shows that the quality factor now represents the ratio of the reactance voltage magnitudes over the voltage v_R across the series resistor R_s. At resonance this voltage equals the terminal voltage v. With one terminal grounded, the potential at the interconnection between the inductor and the capacitor becomes Q times as high as the potential at the driving terminal. This fact may significantly influence the practical realization of high Q series circuits.

Like the parallel circuit in steady state resonance, a constant amount of energy is exchanged between the capacitor and the inductor in the series circuit. In terms of energy there are no differences between the two types of resonance circuits regarding the quality factor, but the loss calculation must now be detailed as a series loss,

$$Q \;=\; 2\pi \left.\frac{\textit{Energy kept in circuit}}{\textit{Energy loss per cycle}}\right|_{\omega=\omega_0} \;=\; 2\pi\,\frac{L i^2}{T_0 i^2 R_s} \;=\; \frac{L\omega_0}{R_s}\,. \qquad (34)$$

Using the resonance frequency and the quality factor from Eq.(32) the impedance of the series circuit is expressed

$$Z_s(j\omega) \;=\; R_s\,[\,1 + jQ\,\beta(\omega)\,]\,, \qquad \textit{where} \quad \beta(\omega) \;=\; \left(\frac{\omega}{\omega_0} - \frac{\omega_0}{\omega}\right). \qquad (35)$$

The frequency is again accounted for through $\beta(\omega)$, so the impedance and admittance functions become symmetric in logarithmic frequency scales as showed in Fig.12.

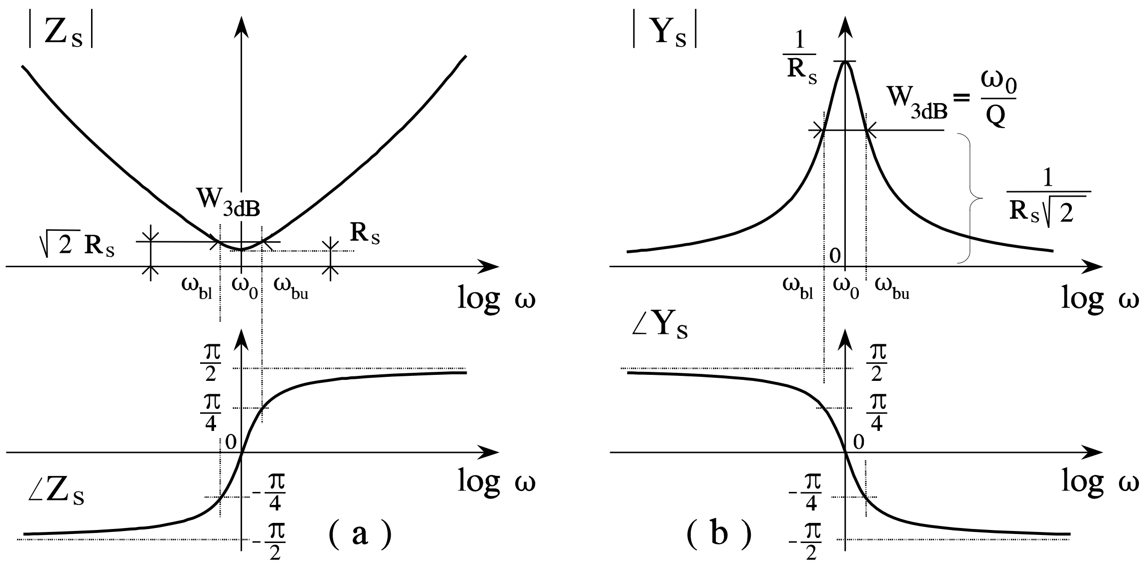

Fig.12 Impedance (a) and admittance (b) magnitudes and phases of the series resonance circuit in Fig.10. The curves are symmetric around ω_o due to the logarithmic frequency scales.

Impedance and admittance magnitudes and phases in Fig.12(a) and (b) are given by

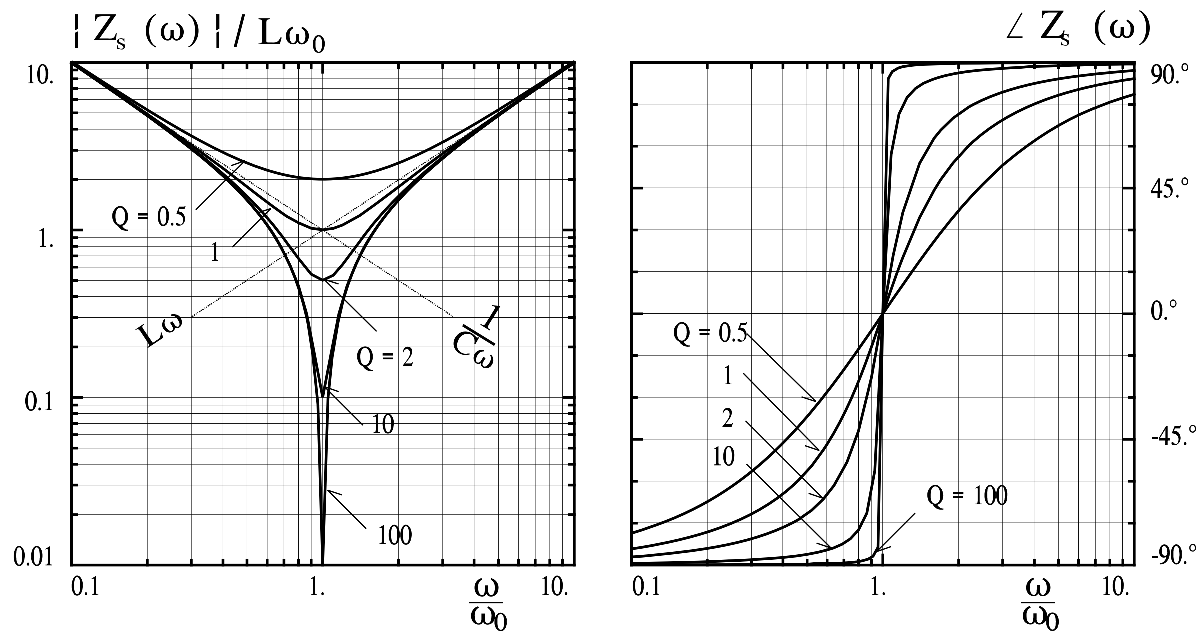

Fig.13 Normalized magnitude and phases for the impedance of series resonance circuits with varying Q-factors.

$$\left| Z_s(j\omega) \right| = R_s \sqrt{1 + Q^2 \beta^2(\omega)}\,, \qquad \angle Z_s(j\omega) = \tan^{-1}\{ Q \beta(\omega) \}\,, \tag{36}$$

$$\left| Y_s(j\omega) \right| = \frac{1}{R_s \sqrt{1 + Q^2 \beta^2(\omega)}}\,, \qquad \angle Y_s(j\omega) = -\tan^{-1}\{ Q \beta(\omega) \}. \tag{37}$$

The equations are equivalent to Eqs.(8) and (7), so all results concerning bandwidth and symmetry of bounds and characteristics may directly be overtaken from the forgoing section. Fig.13 holds impedance characteristics with different Q-factors and shows the asymptotes set by the capacitor and inductor below and above resonance respectively.

Poles and zeros for the series circuits are based on the expressions

$$Z_s(s) = \frac{1}{Y_s(s)} = L\,\frac{s^2 + s\,2\zeta\omega_0 + \omega_0^2}{s} = L\,\frac{s^2 + s\,\omega_0/Q + \omega_0^2}{s}\,. \tag{38}$$

Comparison to Eq.(14) reveals that the zeros of $Z_s(s)$ must follow the pattern of the poles in the parallel circuit while the pole of Z_s in origo corresponds to the zero of Z_p there. In terms of poles and zeros, the series circuit impedance is

$$Z_s(s) = L\,\frac{(s - s_1)\,(s - s_2)}{(s - s_0)}\,, \tag{39}$$

where the geometrical properties of s_0, s_1, and s_2 are the same as in Fig.6.

II-3 Narrowband Approximations

Frequency dependency of the impedance in the parallel resonance circuits was expressed through the nonlinear function β(ω). In consequence, we had to solve 2nd order equations to find prescribed bandlimits. If the circuit is narrowbanded, a linear approximation to the frequency relationship may suffice for design considerations around the resonance frequency. A Taylor expansion provides

$$\beta(\omega) = \left(\frac{\omega}{\omega_0} - \frac{\omega_0}{\omega} \right) \quad \Rightarrow \tag{40}$$

$$\beta(\omega)\big|_{\omega \approx \omega_0} \approx \beta(\omega_0) + \left.\frac{d\beta}{d\omega}\right|_{\omega_0} (\omega - \omega_0) = 0 + \frac{2\,(\omega - \omega_0)}{\omega_0} \,. \tag{41}$$

Following Eq.(9), the 3dB bounds are the frequencies where |Qβ(ω)|=1. With the approximation, bandlimits are placed symmetrically around ω_0, and the 3dB bandwidth becomes

$$\left| \frac{2(\omega_{bu,bl} - \omega_0)}{\omega_0} \right| = \frac{1}{Q} \quad \Rightarrow \quad \omega_{bu} - \omega_0 = \omega_0 - \omega_{bl} = \frac{\omega_0}{2Q} \quad \Rightarrow$$
$$W_{3dB} = \omega_{bu} - \omega_{bl} = \frac{\omega_0}{Q} \,. \tag{42}$$

The same result was obtained in Eq.(10) from the nonlinear β(ω) expression, so the linear approximation gives the right bandwidth. However, Fig.14 reveals that the approximation places the 3dB interval below the correct one. But it is also seen in the figure that the greater Q, the smaller spacing between the 1/Q and -1/Q lines, and the smaller is the error introduced by approximating to symmetrical 3dB bounds through Eq.(41). To quantify this point

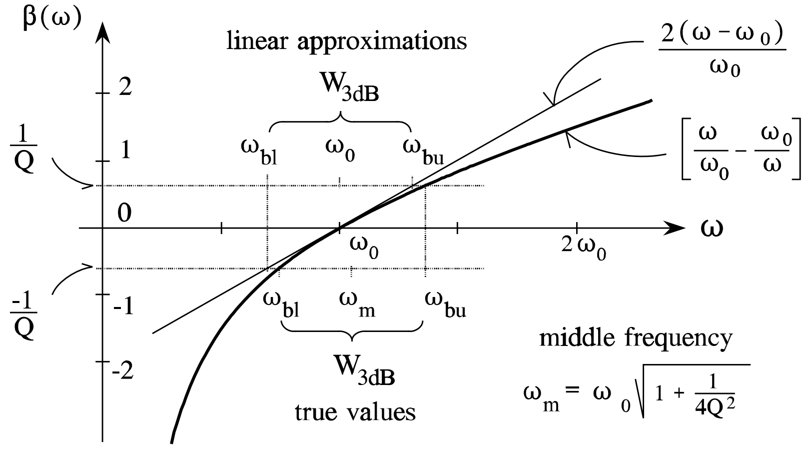

Fig.14 Comparison of true and approximate 3dB bandlimit and bandwidth calculation in simple resonance circuits. The expression for the true middle frequency ω_m is taken from Fig.4.

we calculate the relative difference between the approximated and the true value of the bandlimits. They are equal to the relative difference between the corresponding middle frequencies. It is ω_0 in the linearization while the true middle frequency ω_m depends on Q as indicated by Fig.4. The relative error becomes

$$e_b \equiv \frac{\omega_m - \omega_0}{\omega_0} = \sqrt{1 + \frac{1}{4Q^2}} - 1 \le \begin{cases} 0.1 & : \quad Q \ge 1.09, \\ 0.01 & : \quad Q \ge 3.53, \\ 0.001 & : \quad Q \ge 11.18, \end{cases} \tag{43}$$

The figures show that the accuracy of the approximation is admirable for most applications in circuits where Q is five or more. With Q exceeding one the accuracy may even suffice for initial design estimations.

Inserting the linear expansion of β, the impedance of the parallel resonance impedance circuit is approximated

$$Z_p = \frac{R_p}{1 + jQ\beta} \approx \frac{R_p}{1 + jQ\dfrac{2(\omega - \omega_0)}{\omega_0}} = \frac{R_p}{1 + j\dfrac{(\omega - \omega_0)}{W_{3dB}/2}} . \tag{44}$$

In terms of frequency deviation from resonance, ω-ω_0, the expression is as simple as a first order lowpass characteristic, for instance the impedance of a resistor and a capacitor in parallel as sketched in Fig.15. Thus, instead of the resonance curves in Fig.3 or Fig.5, we may take

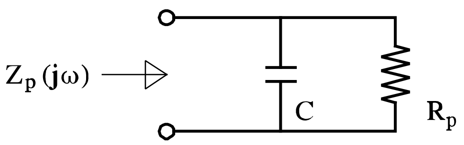

$$Z_p(j\omega) = \frac{R_p}{1 + j\omega/W_{3dB}}$$

$$W_{3dB} = 1 / R_p C$$

Fig.15 Impedance of parallel RC circuit.

the impedance from a normalized first order lowpass characteristics like the one given in Fig.16. Note, however, that compared to the lowpass case of Fig.15, the frequency deviation in the last denominator of Eq.(44) is normalized with respect to half the 3dB bandwidth, because there are 3dB limits on either side of ω_0. The lower frequency bound in lowpass is fixed to zero and not found from an expression. A standardized characteristic as the one in Fig.16 has several interpretations, including

$$\frac{Z_p(j\Omega)}{R_p} = \frac{1}{1 + j\Omega}, \quad \textit{where} \quad \Omega = \begin{cases} \dfrac{\omega}{W_{3dB}} & \sim \textit{lowpass}, \\ Q\beta = \dfrac{\omega_0}{W_{3dB}}\left(\dfrac{\omega}{\omega_0} - \dfrac{\omega_0}{\omega}\right) & \sim \textit{bandpass}, \\ \dfrac{\omega - \omega_0}{W_{3dB}/2} & \sim \textit{bandpass in narrowband approximation}. \end{cases} \tag{45}$$

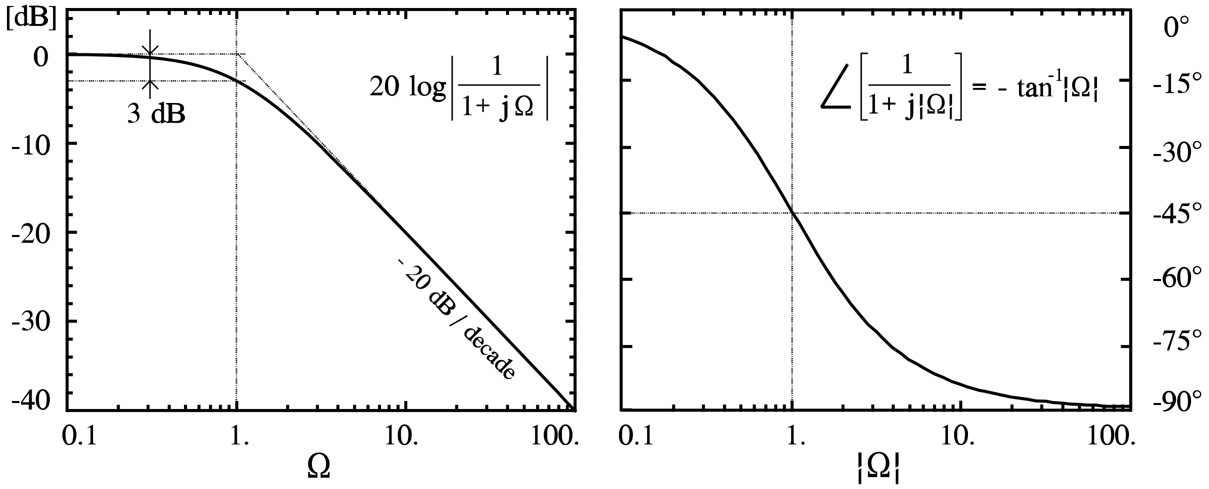

Fig.16 Normalized first order lowpass characteristics. The sign of Ω must precede the phase in bandpass interpretations, either complete or narrowband approximated.

It must still be kept in mind that the narrowband approximation is useful around ω_0, but gives wrong results far from this region. For instance, the true and the approximated bandpass expressions in Eq.(45) are seen to give different results using $\omega = 0$ or $\omega \rightarrow \infty$.

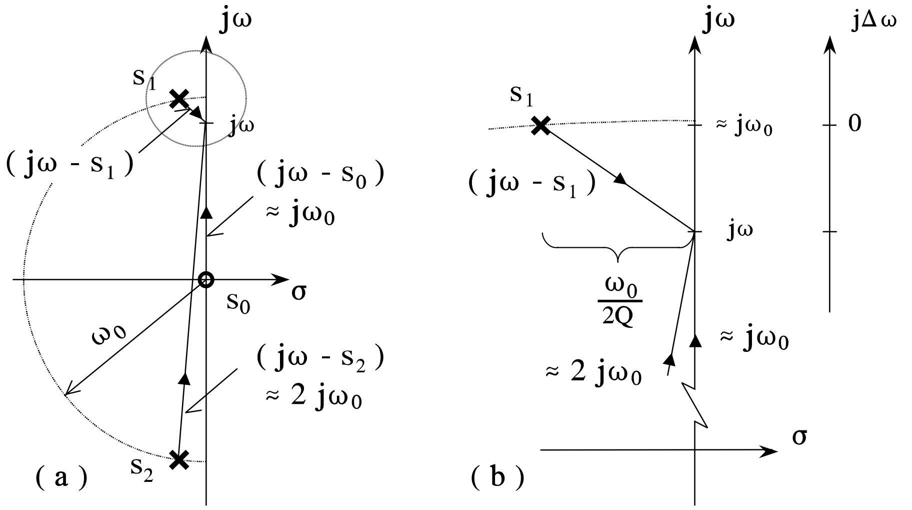

Fig.17 Contributions from poles s_1, s_2 and zero s_0 to Z_p in narrowband approximation where (b) is an expanded view of the encircled region in (a).

Another approach to narrowband approximations takes an outset in the pole and zero constellation. With high Q-values, the poles are close to the imaginary frequency axis. If we limit our scope of investigation to the region around the upper pole, for instance the encircled region in Fig.17, the distances to the other pole s_2 and the zero s_0 are long. As indicated by the figure, their contributions to the impedance are taken constant, $2j\omega_0$ and $j\omega_0$ respectively, so the impedance becomes,

$$Z_p(s) \;=\; \frac{1}{C}\,\frac{\left(s - s_0\right)}{\left(s - s_1\right)\left(s - s_2\right)} \;\approx\; \frac{1}{C}\,\frac{j\,\omega_0}{\left(s - s_1\right)\,j2\,\omega_0} \;=\; \frac{1}{2C\left(s - s_1\right)} \;. \qquad (46)$$

Using the pole position estimates from Eq.(17)(c) and inserting the Q -factor from Eq.(1), the approximation along the imaginary axis s=jω it calculated to yield

$$Z_p(j\omega) \approx \frac{1}{2C}\,\frac{1}{j\omega - j\omega_0 + \dfrac{\omega_0}{2Q}} = \frac{Q}{C\omega_0}\,\frac{1}{1 + jQ\,\dfrac{2(\omega-\omega_0)}{\omega_0}} = \frac{R_p}{1 + j\,\dfrac{\omega-\omega_0}{W_{3dB}/2}} \,. \tag{47}$$

As seen, this is the same impedance approximation that was obtained in Eq.(44) on basis of the Taylor expansion of β(ω). So it is concordant to approximate the impedance function by the last parts Eq.(46) in s-plane calculations or by Eq.(44) along the jω axis.

Simplifications by the narrowband approximations for resonance circuits are beneficial in many computations. Before leaving the subject we shall, however, expand the scope beyond resonance circuits. The frequency dependency of a network is determined through the reactances of capacitors and inductors. Suppose we know a network and its corresponding frequency response H(s). This response may be transformed to another frequency range by mapping frequencies while preserving individual reactances everywhere in the circuit, a technique that is fundamental to filter design [1],[2],[3]. One such mapping - the only one we consider - is the lowpass to bandpass transformation given by

$$s_{lp} \rightarrow s_{bp} + \frac{\omega_0^2}{s_{bp}} \,, \qquad \Rightarrow \qquad \omega_{lp} \rightarrow \omega_{bp} - \frac{\omega_0^2}{\omega_{bp}} = \omega_0\left(\frac{\omega_{bp}}{\omega_0} - \frac{\omega_0}{\omega_{bp}}\right) . \tag{48}$$

Here subscripts "lp" and "bp" are introduced to distinguish between lowpass and bandpass frequency planes. Along the imaginary axes where $s_{lp}=j\omega_{lp}$ and $s_{bp}=j\omega_{bp}$, the transformation agrees with the lowpass and bandpass relations in (45). Applying the transformation directly to circuit components maps inductors and capacitors in lowpass networks to series and parallel resonance circuits in bandpass, where we get

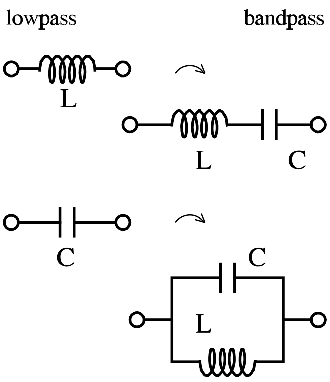

Fig.18 Lowpass-to-bandpass transformation of inductors and capacitors.

$$L\,s_{lp} \rightarrow L\,s_{bp} + L\,\frac{\omega_0^2}{s_{bp}} = L\,s_{bp} + \frac{1}{C\,s_{bp}} \,, \qquad \text{where} \quad C = \frac{1}{L\omega_0^2} \,, \tag{49}$$

$$C\,s_{lp} \rightarrow C\,s_{bp} + C\,\frac{\omega_0^2}{s_{bp}} = C\,s_{bp} + \frac{1}{L\,s_{bp}} \,, \qquad \text{where} \quad L = \frac{1}{C\omega_0^2} \,. \tag{50}$$

If the lowpass response of a network is known in form of a transfer or immitance[3] function $H(s)=H(s_{lp})$, the corresponding bandpass expressions, which accounts for the components mappings, is the one obtained replacing s_{lp} by s_{bp}. If the lowpass response is characterized by poles, zeros, or other characteristic complex frequencies, we must solve for s_{bp} in terms of s_{lp} to get the corresponding bandpass properties, i.e.

$$s_{lp} = s_{bp} + \frac{\omega_0^2}{s_{bp}} \qquad \Rightarrow \qquad s_{bp} = \frac{s_{lp}}{2} \pm \sqrt{\frac{s_{lp}^2}{4} - \omega_0^2} \ . \tag{51}$$

A major reason to consider the lowpass to bandpass transformation is the fact that many common, renowned frequency characteristics[4] are described as lowpass prototypes. To use them in bandpass circuits, we must use the lowpass to bandpass transformation. If the transformation is based on pole-zero patterns, Eq.(51) must be employed. A center frequency in bandpass, which is large compared to the bandwidth in translation, imply the simplified solution

$$s_{bp} \underset{|\,s_{lp}\,| \ll \omega_0}{\approx} \frac{s_{lp}}{2} \pm j\,\omega_0 \ . \tag{52}$$

If the approximation applies, we have narrowband conditions. Here, a lowpass pole-zero pattern around origo described by positions s_{lp} in the lowpass s-plane transforms to bandpass by copying two linearly scaled versions of the patterns, one centering at $j\omega_0$ and one at $-j\omega_0$. This is clearly much simpler than solving for the correct poles and zeros through Eq.(51). Example II-5-2 in the next section discusses the question further. Like other narrowband considerations the simplifications remain valid with poles and zeros close to the lowpass origin or the bandpass centers. Far apart the true solution must still be employed, in particular with respect to the zeros at infinity that are inherent properties of the lowpass characteristic. Zeros at infinity means that the power of s_{lp} in the transfer function denominator is higher than the power in the numerator. By Eq.(51) the lowpass plane point of infinity maps to two zeros in bandpass, one at infinity and one in origo. The latter are not encompassed by the narrowband approximation. It must be separately accounted for if the approximation method is used to realize bandpass circuits.

3) Immitance is a collective name for impedance and admittance.

4) Names like Butterworth, Chebyshev, Legendre, and Cauer or features like elliptic or equal-ripple are examples.

II-4 Series-to-Parallel Conversions

Many practical situations include resonant circuits that are not ideal parallel or series circuits. Clearly, it is always possible to elaborate impedance or transfer function expressions in full details for the particular circuits in question. At single frequencies or under narrow-band conditions, however, a technique known as series-to-parallel conversion may greatly simplify the efforts to get useful results while keeping major insight on the circuit performance. Due to the frequent - but often tacit - use of the method in technical literature and data sheets, its foundation is presented here in some details.

Fig.19 and Fig.20 show a series connection and a parallel connection of a resistance and a reactance. The resultant impedances and admittances are given in Eqs.(53),(54) and (55),(56) respectively.

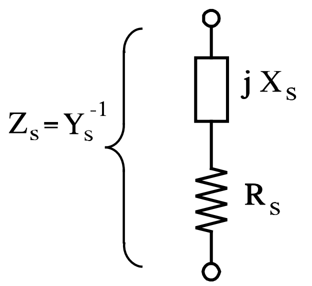

Fig.19

$$Z_s = R_s + jX_s = Y_s^{-1} , \tag{53}$$

$$Y_s = \frac{1}{R_s + jX_s} = \frac{R_s - jX_s}{R_s^2 + X_s^2} , \tag{54}$$

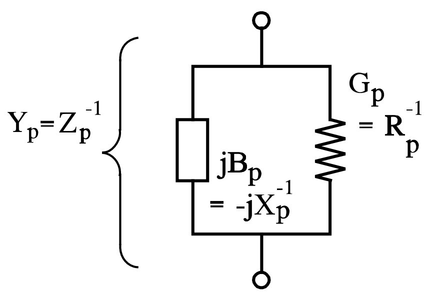

Fig.20

$$Y_p = G_p + jB_p = 1/R_p - j/X_p = Z_p^{-1} , \tag{55}$$

$$\begin{aligned} Z_p &= \frac{jR_pX_p}{R_p + jX_p} = \frac{jR_pX_p(R_p - jX_p)}{R_p^2 + X_p^2} \\ &= \frac{R_pX_p^2}{R_p^2 + X_p^2} + \frac{jX_pR_p^2}{R_p^2 + X_p^2} . \end{aligned} \tag{56}$$

Forcing agreement between the two admittances gives the series-to-parallel conversions, i.e. resistance and reactance conditions by which the parallel connection in Fig.20 may replace the series connection in Fig.19.

$$Y_s = Y_p \quad \Rightarrow \quad R_p = \frac{R_s^2 + X_s^2}{R_s} , \quad and \quad X_p = \frac{R_s^2 + X_s^2}{X_s} . \tag{57}$$

Similarly, equating impedances gives the parallel-to-series conversions,

$$Z_p = Z_s \Rightarrow \qquad R_s = \frac{R_p X_p^2}{R_p^2 + X_p^2} \;, \qquad and \quad X_s = \frac{X_p R_p^2}{R_p^2 + X_p^2} \;. \tag{58}$$

If reactance is the dominating contribution to the impedance in consideration, that is either $R_s \ll |X_s|$ in series or $R_p \gg |X_p|$ in parallel connections, the two types of conversion simplify to the approximations

$$\left.\begin{matrix} R_s^2 \ll |X_s|^2 \\ R_p^2 \gg |X_p|^2 \end{matrix}\right\} : \quad R_p \approx \frac{X_s^2}{R_s} \qquad or \quad R_s \approx \frac{X_p^2}{R_p} \qquad and \qquad X_p \approx X_s \;, \tag{59}$$

The last expressions are the ones most commonly associated with the concept of parallel-to-series conversion. In this form they are particularly easy to memorize due to the symmetry of converting back and forth between series and parallel representations. The following example illustrates the technique of using the series-to-parallel method directly in design.

Example II-4-1 (impedance matching)

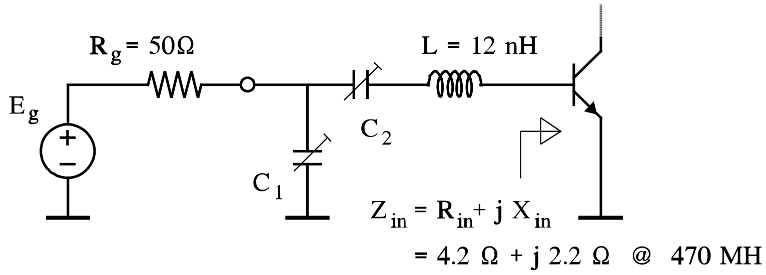

Fig.21

A power transistor of known input impedance should match a 50Ω generator at 470 MHz using the circuit in Fig.21, where biasing components are left out. Inductor L is fixed and C_1, C_2 are trimmer capacitors. Find the trimmer settings and estimate the half power bandwidth of transfer to the transistor.

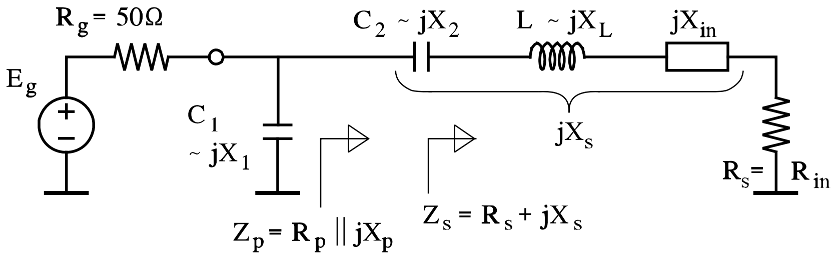

Fig.22

To solve the problem we consider the equivalent circuit in Fig.22. A basic requirement for matching is $R_p = R_g$, so the mapping of R_{in} to parallel form through the combined series reactance X_s must equal R_g. When the required X_s is found, capacitor C_1 is adjusted to tune out the corresponding parallel reactance X_p by setting X_1=-X_p. Using terms from the figure and the simplified conversions from Eq.(59), where X_p=X_s , we get

$$R_p = \frac{X_s^2}{R_{in}} \quad \Rightarrow \quad X_s = \sqrt{R_p R_{in}} = \sqrt{50 \cdot 4.2} = 14.49\,\Omega \tag{60}$$

$$X_L = 2\pi\ 470 \cdot 10^6\ 12 \cdot 10^{-9} = 35.44\,\Omega\,, \tag{61}$$

$$\begin{aligned} X_2 &= \frac{-1}{C_2\,\omega} = X_s - X_L - X_{in} = 14.49 - 35.44 - 2.2 = -23.15\,\Omega\,, \\ C_2 &= \frac{1}{\omega\,|X_2|} = \frac{1}{2\pi \cdot 470 \cdot 10^6\ 23.15} = \underline{14.63\,pF}\ . \end{aligned} \tag{62}$$

$$X_1 = \frac{-1}{C_1\,\omega} = -X_s \quad \Rightarrow \quad C_1 = \frac{1}{2\pi\,470 \cdot 10^6\ 14.50} = \underline{23.35\ pF}\,. \tag{63}$$

The value of X_s in Eq.(60) may seem marginal with respect to the prerequisites of the simplified method. Without any assumptions about sizes of impedances, Eqs.(57),(58) provide correspondingly

$$R_p = \frac{X_s^2 + R_{in}^2}{R_{in}} \quad \Rightarrow \quad X_s = \sqrt{R_{in}R_p - R_{in}^2} = \sqrt{50 \cdot 4.2 - 4.2^2} = 13.87\,\Omega \tag{64}$$

$$\begin{aligned} X_2 &= \frac{-1}{C_2\,\omega} = X_s - X_L - X_{in} = 13.87 - 35.44 - 2.2 = -23.77\,\Omega\,, \\ C_2 &= \frac{1}{\omega\,|X_2|} = \frac{1}{2\pi\ 470 \cdot 10^6\ 23.77} = \underline{14.25\,pF}\ . \end{aligned} \tag{65}$$

$$\begin{aligned} X_p &= \frac{X_s^2 + R_{in}^2}{X_s} = \frac{13.87^2 + 4.2^2}{13.87} = 15.14\ \Omega \quad \Rightarrow \\ C_1 &= \frac{1}{\omega\,X_p} = \frac{1}{2\pi\,470 \cdot 10^6\,15.14} = \underline{22.36\,pF}\,. \end{aligned} \tag{66}$$

As seen only small changes follow from the more elaborate but correct conversions. To estimate the bandwidth for power transfer, we consider the network as a parallel resonance circuit and divide it into a capacitive and an inductive side as sketched in Fig.23. At the center frequency the whole available power from the generator is transferred to the transistor since there are no resistive losses in between. Therefore, the network determined above implies conjugated matching across the cut. The parallel resistance R_{pp}, obtained by converting R_{in} to parallel form through inductances only, must be equal to the parallel resistance, which

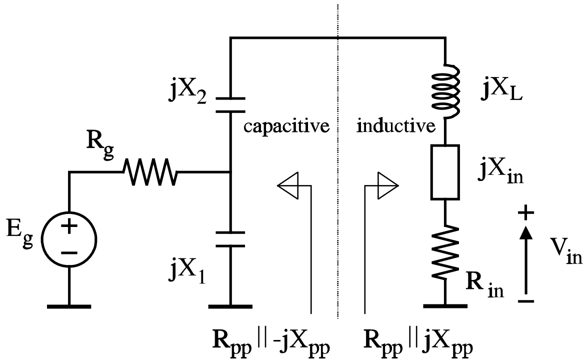

Fig.23

originates from R_g and converts through the capacitive side. In a parallel resonance circuit the Q-factor is the ratio of the total parallel resistance, here ½R_{pp}, over either the inductive or the capacitive reactances. Continuing the simplified approach from Eqs.(60) to (63), which here implies $X_{pp} = X_L + X_{in}$, we get

$$R_{pp} = \frac{(X_L + X_{in})^2}{R_{in}} \,, \qquad Q = \frac{R_{pp}/2}{X_L + X_{in}} = \frac{X_L + X_{in}}{2R_{in}} = \frac{35.45 + 2.2}{2 \cdot 4.2} = 4.481 \tag{67}$$

$$BW_{3dB} = \frac{f_0}{Q} = \frac{470\,MHz}{4.481} = \underline{105.\ MHz}\,.$$

Due to losslessness, the absolute level of the voltage transfer function at the center frequency is most easily calculated letting R_{in} consume the available power, i.e.

$$\frac{v_{in}^2}{R_{in}} = \frac{E_g^2}{4R_g} \quad \Rightarrow \quad \left.\frac{v_{in}}{E_g}\right|_{470MHz} = \frac{1}{2}\sqrt{\frac{R_{in}}{R_g}} = \frac{1}{2}\sqrt{\frac{4.2}{50}} = 0.150 \sim -16.8dB. \tag{68}$$

This quantity wasn't actually asked for, but now it possible to compare our results with simulations as it is done in Fig.24. The fully drawn curve is calculated using capacitances from the simplified method from Eqs.(62),(63) while the dotted curve is based on Eqs.(65),(66). The observable consequence of the simplified method is a slight displacement of the

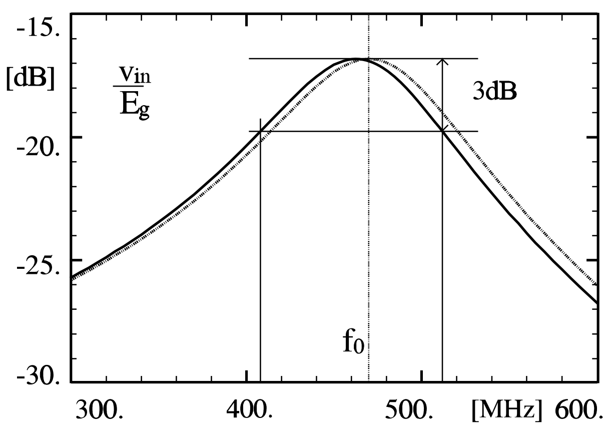

Fig.24

center frequency where matching is obtained. However, the differences in capacitance values between the two situations are easily compensated with trimmer capacitors.

One final point should be observed concerning the bandwidth estimation. The transistor impedance to be matched was taken from data-sheets, and the positive reactance part was treated by Eq.(66) like an inductor for bandwidth estimations. Here it is a tacit assumption that the input reactance does not change faster than an inductor across our frequency band, i.e. without sensible resonances from the transistor or its mounts. If this occurs, we have no means for estimating bandwidth, but the center frequency matching procedure remains valid, if the transistor data are reliable.

Example II-4-1 end

Conversions in Narrowband Applications

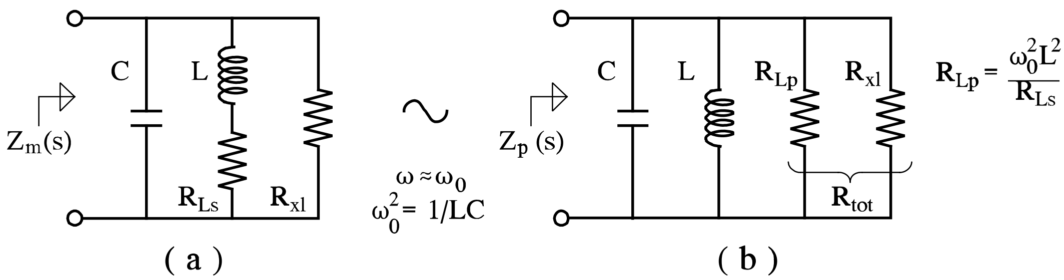

Fig.25 Conversion of a small inductor series resistance R_{Ls} to a parallel resistance R_{Lp} . Circuit (b) is a narrowband approximation to (a) around resonance frequency ω_0.

Reactances of inductors and capacitors depend on frequency so - strictly speaking - a series-parallel conversion applies to a single frequency. However, we could estimate the bandwidth of the resultant circuit in the example above, a consequence of the fact that in narrowband circuits, component values obtained by series-parallel conversions at the center frequency are useable throughout the passband. To see this from an analytical point of view we consider the example in Fig.25. Inductor L is employed in a parallel resonance circuit, but it has a small series resistance R_{Ls}, so the resonance circuit is no longer ideal. To deal with this circuit easily, R_{Ls} is converted to the parallel resistance R_{Lp} and parallel resonance methods are used on the circuit in Fig.25(b). It is supposed that the series resistance is much smaller than the reactance $X_s = L\omega_0$, so the simplified relations from Eq.(68) are used including the fact, that the inductor reactance remains unaffected of the conversion. Therefore, resonance frequency ω_0 is figured out the usual way and the corresponding Q-factor and bandwidth follows from the sequence,

$$\omega_0 = \frac{1}{\sqrt{L\ C}} \quad \Rightarrow \quad R_{Lp} = \frac{X_s^2}{R_{Ls}} = \frac{(\omega_0 L)^2}{R_{Ls}} \quad \Rightarrow \quad R_{tot} = R_{Lp} \parallel R_{xl} = \frac{R_{Lp} R_{xl}}{R_{Lp} + R_{xl}} \quad \Rightarrow$$
$$Q_{tot} = \omega_0 C R_{tot} \quad \Rightarrow \quad W_{3dB} = \frac{\omega_0}{Q_{tot}} \ . \tag{69}$$

Notice that the contributions from the two resistors to the resultant Q-factor are distinguishable through a "parallelling" relationship

$$\frac{1}{R_{tot}} = \frac{1}{R_{xl}} + \frac{1}{R_{Lp}} \qquad \Rightarrow \qquad \frac{1}{Q_{tot}} = \frac{1}{Q_x} + \frac{1}{Q_L} \,, \qquad \textit{where} \tag{70}$$

$$Q_x = C\,\omega_0\,R_{xl} \,, \qquad Q_L = C\,\omega_0\,R_{Lp} = \frac{R_{Lp}}{L\,\omega_0} = \frac{L\,\omega_0}{R_{Ls}} \,. \tag{71}$$

It is not self-evident that the circuit in Fig.25(b) with frequency independent R_{Lp} may substitute the original circuit across a passband. To convince, the two impedance functions must be compared. The ideal parallel circuit is given by Eq.(14),

$$Z_p(s) = \frac{1}{C}\,\frac{s}{s^2 + s\left[\omega_0/Q_{tot}\right] + \omega_0^2} \,. \tag{72}$$

Casting the impedance of the original circuit in Fig.25(a) into a comparable form we get

$$\begin{aligned} Z_m(s) &= \frac{1}{sC + \dfrac{1}{R_{xl}} + \dfrac{1}{sL + R_{Ls}}} = \frac{1}{C}\,\frac{s + R_{Ls}/L}{s^2 + s\left[\dfrac{1}{CR_{xl}} + \dfrac{R_{Ls}}{L}\right] + \dfrac{1}{LC}\left[1 + \dfrac{R_{Ls}}{R_{xl}}\right]} \\ &= \frac{1}{C}\,\frac{s - s_{m0}}{s^2 + s\,\omega_{m0}/Q_m + \omega_{m0}^2} \,. \end{aligned} \tag{73}$$

Identification of Q-factor through the first order denominator term gives

$$\frac{\omega_{m0}}{Q_m} = \frac{1}{CR_{xl}} + \frac{R_{Ls}}{L} \qquad \Rightarrow \qquad \frac{1}{Q_m} = \frac{1}{C\,\omega_{m0}R_{xl}} + \frac{R_{Ls}}{L\,\omega_{m0}} \,, \tag{74}$$

which agrees with the subdivision of Q_{tot} in Eq.(71), provided that the resonance frequencies ω_{m0} and ω_0 are equal. But this is not so unless the resistors meet the condition

$$\omega_{m0}^2 = \frac{1}{LC}\left[1 + \frac{R_{Ls}}{R_{xl}}\right] \approx \omega_0^2 \qquad \Rightarrow \qquad \frac{R_{Ls}}{R_{xl}} \ll 1 \qquad \textit{or} \qquad \frac{R_{xl}}{R_{Ls}} \gg 1 \,. \tag{75}$$

Implicitly the inequalities express a narrowband assumption. The result of a parallel connection cannot exceed any of its components. If $Q_m = Q_{tot} \gg 1$ we must therefore require

$$Q_x \gg 1 \quad and \quad Q_L \gg 1 \quad \Rightarrow \quad Q_x Q_L = C\omega_0 R_{xl} \frac{L\omega_0}{R_{Ls}} = \frac{R_{xl}}{R_{Ls}} \gg 1 \ . \tag{76}$$

Under narrowband conditions the two circuits in Fig.25 will have the same poles because the impedance functions get the same denominators. Regarding numerators Eq.(74) shows that $Z_m(s)$ has a zero on the negative real axis compared to the zero in origo for $Z_p(s)$. Therefore, the impedance Z_m reduces correctly to the parallel combination $R_{Ls} \| R_{xl}$ at dc while the inductor short-circuits in the narrowband approximation.

$$zero|_{Z_m}: \ s_0 = -R_{Ls}/L \ , \qquad Z_m(0) = \frac{1}{C} \frac{R_{ls}}{L\omega_0^2 \left[1 + R_{Ls}/R_{xl}\right]} = \frac{R_{Ls}R_{xl}}{R_{Ls}+R_{xl}} = R_{Ls} \| R_{xl}. \tag{77}$$

Observe, however, that the difference in zeros between Z_m and Z_p is an asymptotic deviation outside the scope of the narrowband assumption. If the response is dominated by poles, which is the case in the passband, the parallel circuit obtained by series-to-parallel conversion at ω_0 is usable to the same degree of confidence that accompanied other types of narrowband approximations.

Parallelling of Q-factor contributions has wider implication than just being a vehicle in the previous discussion. Imperfections in reactive components that cause loss of power may be specified in data sheets or measurements by associating a quality factor directly to the component. In agreement with Eq.(71), the Q-factor is either the ratio of the reactance over a series loss resistance or the ratio of a parallel loss resistance over the reactance. With higher Q´s, say three or more, it makes no difference for narrowband computations whether the physical loss originates in series, parallel, or combined connection, we convert to the form most suited for the problem at hand through the approximate conversion from Eq.(59),

$$R_p = Q_{L,C}\left|X_{L,C}\right|, \quad R_s = \frac{|X_{L,C}|}{Q_{L,C}} \quad \Rightarrow \quad R_p R_s = X_{L,C}^2 \ , \quad X_{L,C} \underset{\substack{ideal\\components}}{=} \begin{cases} L\omega \, , \\ -1/C\omega \ . \end{cases} \tag{78}$$

The combination of Q-factors is sometimes expressed in a terminology of loaded, unloaded, and external Q´s, which follows the paralleling expression, cf.[4] sec.7.1,

$$\frac{1}{Q_{loaded}} = \frac{1}{Q_{external}} + \frac{1}{Q_{unloaded}} \qquad \Rightarrow \qquad Q_{loaded} \le \ \min\left\{ Q_{external}, \ Q_{unloaded} \right\} , \tag{79}$$

Subscript "unloaded" refers to unavoidable loss components in the reactances that make the resonator and "external" to all other resistors. The resultant "loaded" Q determines the bandwidth around resonance and is always smaller than any component Q-factor. In this terminology the example from Fig.25 and Eq.(71) should read

$$Q_{loaded} = Q_{tot} \ , \qquad Q_{external} = Q_{xl} \ , \qquad Q_{unloaded} = Q_L \ . \tag{80}$$

Conversions in Broadband Modeling

In narrowband applications of reactive components it suffices to specify its reactance and Q-factor as a function of frequency. Then we may use Eq.(78) and the series-parallel conversion around the center frequency to make design calculations. On the contrary characterization of reactive components for broadband application, including modelling by frequency independent circuit elements, requires detailed equivalent circuits. To find the models we may still benefit from the series-parallel relationships. The following example illustrates this aspect.

Example II-4-2 (spiral inductor)

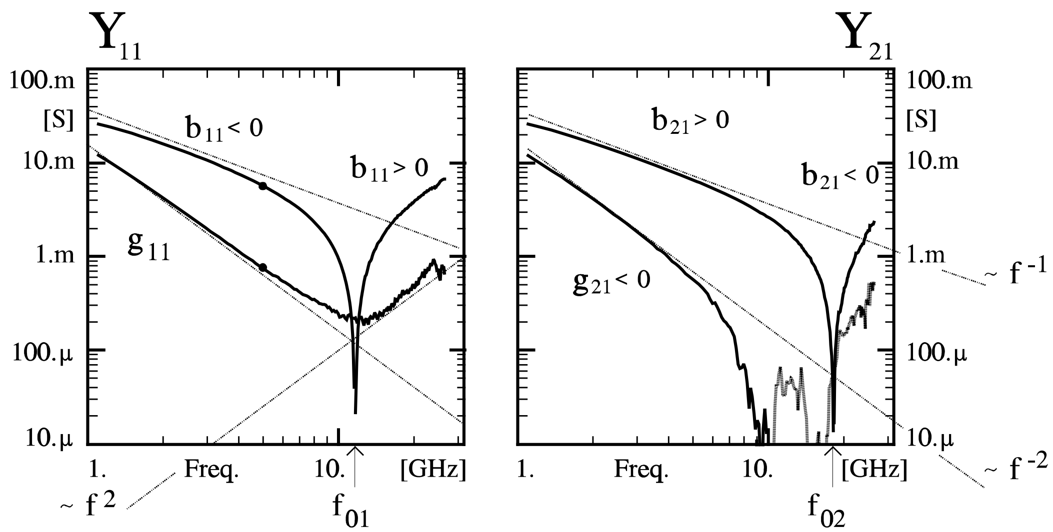

Fig.26 Spiral inductor forward y-parameters. Reverse y_{12} and y_{22} are similar. Data are converted from s-parameter measurements. g_{21}´s are uncertain at high frequencies.

Data from an inductor in a GaAs microwave integrated circuit are shown in Fig.26. The layout is a planar spiral of the type in Fig.27 and the measurements are made with the inductor connecting an input and an output port. Due to small dimensions, thin metal and isolation layers, the inductor is far from being ideal. We wish to find an equivalent circuit based on the measurements. Like other integrated passive component a Π-structured model is expected, so it is natural to translate the experiments to y-parameters. The definitions in forward measurements take form of input and transfer admittances with shorted output as summarized by Fig.28.

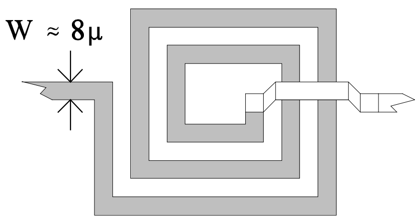

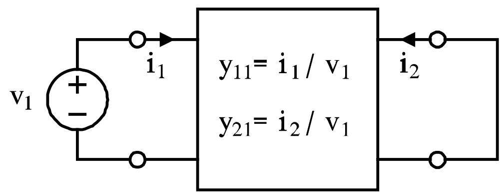

Fig.27 Spiral inductor layout example. Fig.28 Definition of y-parameters y_{11}, y_{21}.

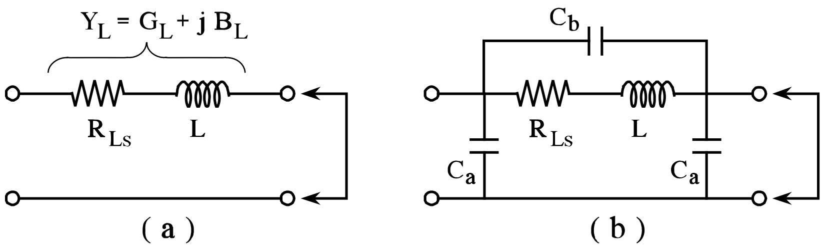

Fig.29 Spiral inductor equivalent circuit where (a) suffices below the resonances that are included by (b). The shorts at the outputs are required to interpret y-parameters.

Fairly below 10 GHz the data show nearly ideal asymptotic behavior, where imaginary and real parts are inversely proportional to frequency or squared frequency respectively. The latter indicates that the dominant inductor loss is a series loss. To see this we convert the simple equivalent circuit in Fig.29(a) to y-parameter parallel form through

$$y_{11} = g_{11} + jb_{11} = Y_L \,, \quad y_{21} = g_{21} + jb_{21} = -Y_L \,, \qquad where$$
$$Y_L = G_L + jB_L = \frac{1}{R_{Ls} + jL\omega} \approx \frac{R_{Ls}}{(L\,\omega)^2} - j\,\frac{1}{L\,\omega} \,. \tag{81}$$

The real conductance component shows the observed second order relationship. Extrapolating the declining asymptotes to the frame of the figures at 31.62 GHz gives

$$|B_L|_{31.62GHz} = 1.11mS \;\Rightarrow\; L = \left|\frac{1}{\omega B_L}\right| = \frac{1}{2\pi\,31.62\cdot 10^9\,1.11\cdot 10^{-3}} = \underline{4.53nH} \,,$$
$$G_L|_{31.62GHz} = 15.8\,\mu S : \; G_L = \frac{R_{Ls}}{(L\omega)^2} = R_{Ls}B_L^2 \;\Rightarrow\; R_{Ls} = \frac{G_L}{B_L^2} = \frac{15.8\cdot 10^{-6}}{1.11^2\cdot 10^{-6}} = \underline{12.8\,\Omega} \,. \tag{82}$$

The series resistance is high and troubles many designs using integrated spiral inductors. At 5GHz, for instance, the experimental data (dots in Fig.26) are close to the maximum Q-factor, which develops

$$Q_L\Big|_{5.GHz} = \frac{L\omega}{R_{Ls}} = \frac{R_{Lp}}{L\omega} = \left|\frac{B_L}{G_L}\right| = \left|\frac{b_{11}}{g_{11}}\right| = \frac{5.9mS}{0.73mS} = 8.1 \,. \tag{83}$$

Above 10 GHz the data indicate resonances in both y-parameters. The susceptances of the inductance are here canceled by stray capacitors, at f_{01}=11.52 GHz in y_{11} and at f_{02}=18.16 GHz in y_{21}. To include resonances the model is enhanced to Fig.29(b), which now gives

$$y_{21} = -Y_L - j\omega\,C_b \;:$$
$$2\pi f_{02} = \frac{1}{\sqrt{L\,C_b}} \;\Rightarrow\; C_b = \frac{1}{\omega_{02}^2 L} = \frac{1}{(2\pi\,18.16\cdot 10^9)^2 4.53\cdot 10^{-9}} = \underline{16.95fF} \,, \tag{84}$$

$$y_{11} = Y_L + j\,\omega\left(C_a + C_b\right):$$

$$2\pi f_{01} = \frac{1}{\sqrt{L\left(C_a + C_b\right)}} \quad\Rightarrow\quad C_a + C_b = \frac{1}{\omega_{01}^2 L} = \frac{1}{(2\pi\, 11.52\cdot 10^9)^2 4.53\cdot 10^{-9}} = 42.13 fF, \tag{85}$$

$$C_a = 42.12\,fF - 16.95\,fF = \underline{25.18\,fF}\;. \tag{86}$$

A final look at the measurements shows a distinct asymptote in the real part of y_{11} above resonance f_{01}. The asymptote increases in proportion to the squared frequency, which might be the effect of a small resistance in series with a capacitor. It is therefore tempting to make

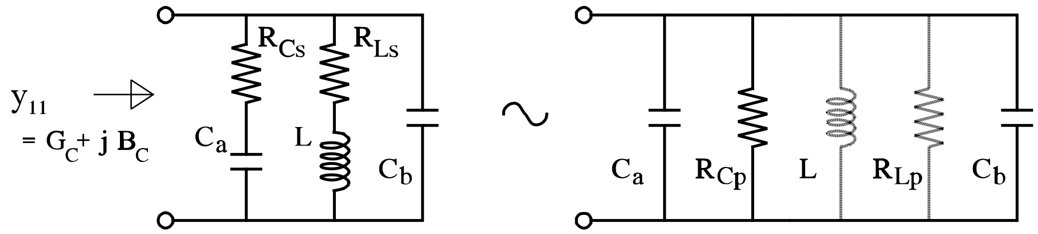

Fig.30 Complete y_{11} model and the elements that are sensed above resonance.

one more step in the modeling. Considering y_{21}, the real parts of the experimental data are too noisy and uncertain for further identifications, and we concentrate on y_{11} as shown in Fig.30. Now the asymptote for g_{11} at the frame of the data implies

$$G_C\big|_{31.62\,GHz} = 0.92\,mS:$$

$$G_C = \frac{1}{R_{Cp}} = R_{Cs} C_a^2\,\omega^2 \;\Rightarrow\; R_{Cs} = \frac{G_C}{C_a^2\omega^2} = \frac{0.92\cdot 10^{-3}}{\left(25.18\cdot 10^{-15}\cdot 2\pi\, 31.62\cdot 10^9\right)^2} = \underline{36.8\ \Omega}\;. \tag{87}$$

Including the last extension, the equivalent circuit for the spiral inductor takes the shape of Fig.31. The y-parameters, which this model accounts for, are shown in Fig.32. The only observable discrepancies to the measurements are in g_{21} above resonance, where the experi-

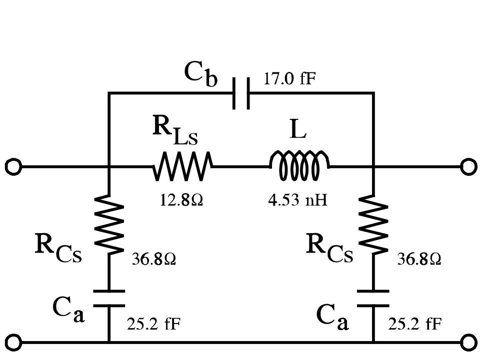

Fig.31 Complete equivalent for the spiral inductor measurements.

mental data are badly conditioned. In view of literature on GaAs IC design, for instance [5], the model we have constructed from nothing but basic knowledge on series-parallel transformations and resonance circuits is rather complete.

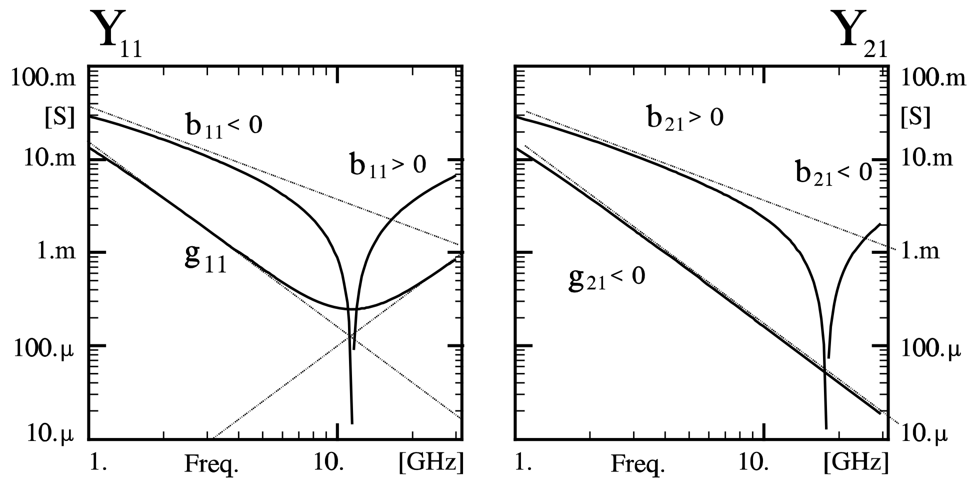

Fig.32 Simulated verification of the complete spiral inductor equivalent circuit from Fig.31. The corresponding experimental data were shown in Fig.26.

Example II-4-2 end

II-5 Tuned Amplifiers

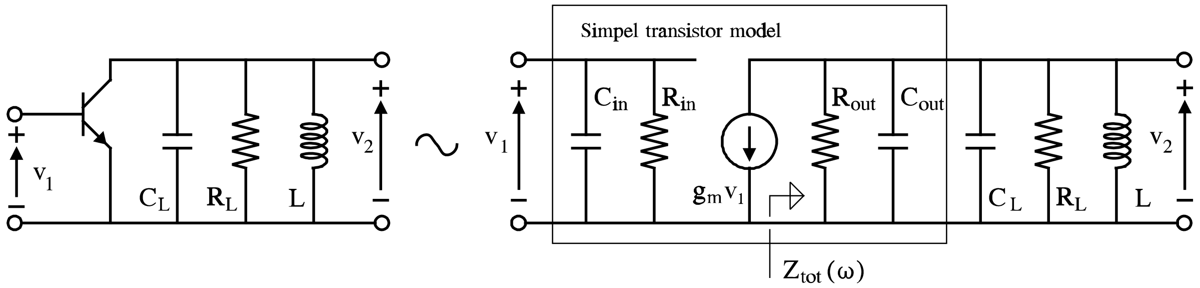

Fig.33 Functional and simplified equivalent circuit of a single-tuned amplifier.

Resonance circuits are used to shape the frequency response of frequency selective amplifiers. Fig.33. shows an example where a bipolar junction transistor is loaded by a parallel resonance circuit. A simple transistor equivalent circuit is employed to keep the amplification function uncomplicated. Using Eq.(45) the voltage gain v_2/v_1 is expressed

$$A(j\omega) = \frac{v_2}{v_1} = -g_m Z_{tot}(j\omega) = \frac{-g_m R_{tot}}{1 + j\,\Omega(\omega)} = \frac{A_0}{1 + j\,\Omega(\omega)} . \tag{88}$$

The transistor output capacitance and conductance add to the external tuning circuit components to give center frequency amplification A_0 and bandwidth,

$$A_0 \equiv A(j\omega_0) = -g_m R_{tot} , \qquad R_{tot} = R_L \parallel R_{out} , \qquad C_{tot} = C_{out} + C_L$$

$$\omega_0 = \frac{1}{\sqrt{L\,C_{tot}}} , \qquad Q_{tot} = R_{tot}\,\omega_0\,C_{tot} , \qquad W_{3dB} = \frac{\omega_o}{Q_{tot}} = \frac{1}{R_{tot}C_{tot}} . \tag{89}$$

Note, the input resistance and capacitance in the transistor model have no direct effects on these expressions, but play the role of loads if more stages are cascaded. The frequency response, which shapes like the parallel circuit impedance function $Z_{tot}(j\omega)$, may be calculated either fully correct or narrowband approximated by the frequency expressions

$$\Omega(\omega) = \frac{\omega_0}{W_{3dB}}\left(\frac{\omega}{\omega_0} - \frac{\omega_0}{\omega}\right) \underset{Q_{tot} \gg 1}{\approx} \frac{(\omega - \omega_0)}{W_{3dB}/2} . \tag{90}$$

Recall from the discussion on the narrowband approximation in section II-3 that the two forms differ with respect to bandlimits but not bandwidths.

To compare frequency selective amplifiers, two figures of merits are the gain-bandwidth product and the gain-bandwidth factor. The product is defined as the center frequency voltage gain times the 3dB bandwidth,

$$GW \equiv \left| \textit{center freq. voltage gain} \right| \times \textit{3dB-bandwidth}[rad/\sec] = \left| A_0 \right| W_{3dB} . \tag{91}$$

With more stages the GW-product commonly refers to an average gain per stage, i.e. [5]

$$GW_{av} \equiv \left| center\ freq.\ voltage\ gain \right|^{1/N} \times 3dB\text{-}bandwidth\,[rad/\mathrm{sec}] = \left| A_{N0} \right|^{1/N} W_{3dB}\,, \tag{92}$$

where N is the number of tuned stages. The single stage amplifier above has

$$GW \equiv \left| A_0 \right| W_{3dB} = g_m / C_{tot}\ . \tag{93}$$

This product is used as a reference for the gain-bandwidth factor, GBF, which is defined by

$$GBF \equiv \frac{GW_{av}}{g_m / C_{tot}}\ . \tag{94}$$

It is supposed, that the transconductance and the total loading capacitance are the same in both numerator and denominator. Transconductance g_m is a property of the transistor. In the lower limit C_{tot} holds the transistor output capacitance and other unavoidable contributions from mounts and loads. Therefore, GW is often used as a goal for optimizing or comparing transistor and IC performances. The normalized GBF is suited for comparing amplifier structures without detailed regards to the devices that give the gain.

There exists a series of fundamental theorems concerning GBF's of interstage connections between amplifier stages, first introduced by Bode [6]. Their derivations and detailed interpretations are beyond the present scope and needs. Briefly, when one amplifier stage is connected to the next, it is stated that GBF cannot exceed two with a passive one-port paralleled across the connection. A passive two-port interstage coupling has a theoretical maximum of four. Networks representing the maxima are complicated and of little practical use with the high gain RF transistors of today. However, it is still informative to use GBF in comparisons between different amplifier structures even when they fall considerably below the theoretical limits.

An amplifier stage holding only one resonance circuit is called a single-tuned amplifier. With more resonance circuits separated by transistors there are many possibilities on how to organize their center frequencies and Q-factors. The simplest case is that all tuning circuits have identical resonance properties. This well-defined situation is called synchronous tuning, as opposed to a more diversified group of so-called stagger tuned amplifiers.

---

5) There are many competing definitions and notations around. Bandwidth in units of radians per second is denoted GW here, while GBW is used if bandwidths are in units of Hz. The term MGBW - "M" for mean - may be seen instead of GW_{av}.

Synchronously Tuned Amplifiers

Cascading N equally tuned amplifier stages of the type from Fig.33 gives a voltage amplification of form,

$$A_N(j\omega) = \frac{A_{N0}}{(1 + j\Omega)^N} , \qquad A_{N0} = A_{10}\, A_{20} \cdots A_{n0} , \tag{95}$$

The center frequency amplification A_{N0} at $\Omega = 0$ is the product of the center frequency amplifications in each stage. In normalized frequency a single stage amplifier has 3dB bandlimits corresponding to $\Omega=\pm 1$. With N equally tuned stages we must solve for the Ω's that reduces the absolute amplification by a factor of $\sqrt{2}$, that is

$$\Omega_{bl} : \quad \left| \frac{A(\Omega_{bl})}{A_{N0}} \right|^2 = \frac{1}{\left(1 + \Omega_{bl}^2\right)^N} = \frac{1}{2} \quad \Rightarrow \quad \Omega_{bl} = \sqrt{2^{1/N} - 1} . \tag{96}$$

Without normalization with respect to frequency, the result gives the bandwidth of N stages in terms of one stage through

$$W_{3dB}\Big|_{N\ stages} = GBF_N \times W_{3dB}\Big|_{one\ stage} , \qquad GBF_N = \sqrt{2^{1/N} - 1} , \tag{97}$$

where the gain-bandwidth factor GBF_N in this particular application also is called the bandwidth reduction or bandwidth shrinkage factor. Examples of the reduction process are

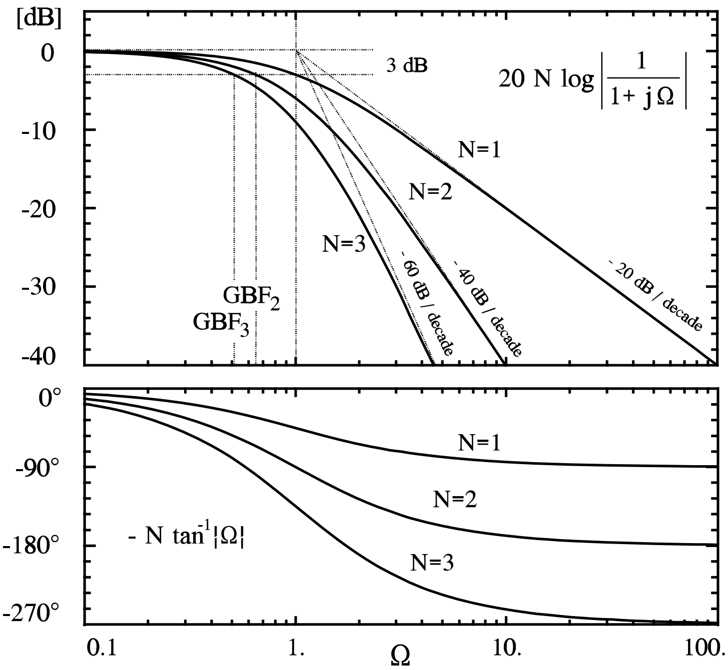

Fig.34 Normalized amplitude and phase characteristics in synchronous tuning. Gain-bandwidth factors GBF_2, GBF_3 give the bandwidth reductions for 2 and 3 stages.

seen in the characteristics of Fig.34. The amplitude of N equally tuned stages rolls off approaching an asymptote of -N×20dB/decade. The stronger the bending of the corresponding curve, the smaller becomes the bandwidth. Since $2^{1/N} \rightarrow 1$ with growing N , the reduction factor may be approximated from the following estimations,

$$\log(1+x) \approx x \quad for \quad |x| \ll 1 \quad \Rightarrow \quad x \equiv 2^{1/N} - 1 = \left(e^{\log 2}\right)^{1/N} - 1 \approx \frac{\log 2}{N} \ ,$$
$$GBF_N = \sqrt{2^{1/N} - 1} \approx \sqrt{\frac{\log 2}{N}} = \frac{1}{1.20\sqrt{N}} \ . \qquad (98)$$

True and estimated bandwidth reductions are compared below in Table I. Whenever more stages are cascaded, the approximation gives reasonable results.

Table I True and approximated Gain-Bandwidth Factors (Bandwidth Reduction Factors) for N Synchronously tuned amplifier stages.

N	GBF_N	$\sim GBF_N$	N	GBF_N	$\sim GBF_N$
2	0.6436	0.5893	5	0.3856	0.3727
3	0.5098	0.4811	6	0.3499	0.3407
4	0.4350	0.4167	7	0.3226	0.3150

Example II-5-1 (synchronous tuning)

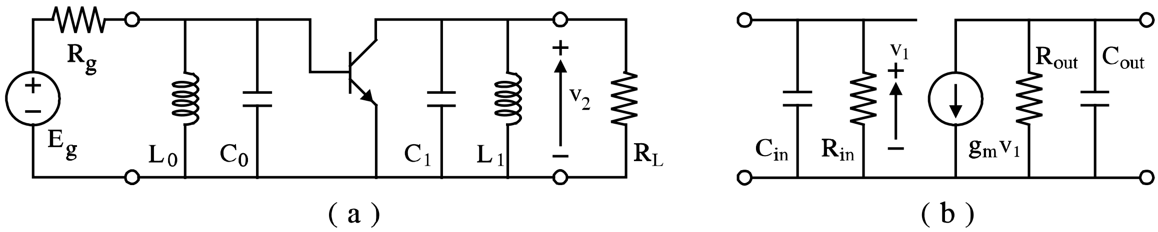

Fig.35 Amplifier principle, (a), and transistor equivalent circuit, (b).

The amplifier in Fig.35(a) should operate with R_g=R_L=75Ω having a total bandwidth in synchronous tuning of BW_{amp}=55 MHz around f_0=460 MHz. Transistor data are

$$g_m = 200\,mS, \quad R_{in} = 520\,\Omega, \quad C_{in} = 6.5\,pF, \quad R_{out} = 12.5\,k\Omega \ , \quad C_{out} = 1.6\,pF \ . \qquad (99)$$

Find the external components C_0, L_0, C_1, L_1, and the center frequency gain v_2/E_g.

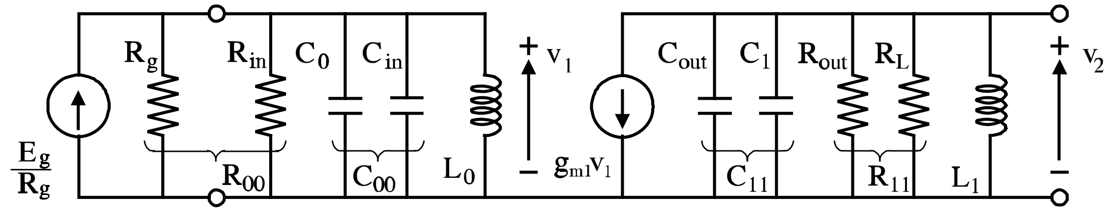

Fig.36

Including the transistor model, a complete functional equivalent circuit for the amplifier becomes the one shown in Fig.36 where the generator is changed to the Norton equivalent.

The two tuned circuits have equal bandwidths BW_0 and quality factors Q_0. Compensating for bandwidth reduction, we get

$$BW_0 = \frac{BW_{amp}}{GBF_2} = \frac{55\,MHz}{.6436} = 85.46\,MHz, \qquad Q_0 = \frac{f_0}{BW_0} = \frac{460\,MHz}{85.46\,MHz} = 5.383 \ . \qquad (100)$$

At the input side, the parallel resistance R_{00} determines the impedance level and in turns give the external components,

$$R_{00} = R_g \| R_{in} = \frac{75 \cdot 520}{75 + 520} = 65.55\,\Omega\,, \qquad \omega_0 = 2\pi f_0 = 6.283 \cdot 460\;10^6 = 2.890\;10^9,$$

$$C_{00} = \frac{Q_o}{\omega_0 R_{00}} = \frac{5.383}{2.890\,10^9 \cdot 65.55} = 28.41\,pF, \qquad C_0 = C_{00} - C_{in} = 28.41 - 6.5 = \underline{21.9\ pF}, \qquad (101)$$

$$L_0 = \frac{1}{\omega_0^2 C_{00}} = \frac{1}{2.890^2\,10^{18}\,28.41\,10^{-12}} = \underline{4.21\ nH}\ .$$

The corresponding calculations at the output side of the transistor read,

$$R_{11} = R_L \| R_{out} = \frac{75 \cdot 12500}{75 + 12500} = 74.55\,\Omega\,,$$

$$C_{11} = \frac{Q_o}{\omega_0 R_{11}} = \frac{5.383}{2.890\,10^9 \cdot 74.55} = 24.98\,pF, \qquad C_1 = C_{11} - C_{out} = 24.98 - 1.6 = \underline{23.4\ pF}, \qquad (102)$$

$$L_1 = \frac{1}{\omega_0^2 C_{11}} = \frac{1}{2.890^2\,10^{18}\,24.98\,10^{-12}} = \underline{4.79\ nH}\ .$$

The inductances we have found here approaches the lower borderline for practical lumped inductors. A guideline is that unwounded wires like component leads have inductances about 0.5nH/mm to 1nH/mm, a result that is verified in chap.4 of ref.[7]. The smallest inductor available as a commercial component for surface mounting on PC-boards is presently 2nH.

The impedances of the tuned circuits are equal to the parallel resistances at the center frequency, so the voltage gain becomes

$$A_0 = \frac{v_2}{E_g} = -\frac{R_{00} g_m R_{11}}{R_g} = -\frac{65.55 \cdot 0.2 \cdot 74.55}{75.} = \underline{-13.0} \qquad (103)$$
$$\sim 20\log_{10}(13.) = 22.3dB \ .$$

The frequency characteristic of the amplifier is shown later in Fig.43.

Example II-5-1 end

The phase characteristic in synchronous tuning with N stages may be written

$$\angle A_N = -N \tan^{-1}(\Omega) = -N \left\{ \Omega - \frac{1}{3}\Omega^3 + \frac{1}{5}\Omega^5 + \dots \right\} , \qquad (104)$$

where the last equation introduces the Taylor expansion of $\tan^{-1}(\Omega)$. Instead of using Ω, which is normalized with respect to the 3dB bandwidth of a single stage, we normalize frequency with respect to the approximate 3dB bandwidth from Eq.(98) for the N stages in consideration. The new frequency variable becomes

$$\Omega_N \equiv \Omega \sqrt{\frac{N}{\log 2}} = \Omega \ 1.20 \sqrt{N} \ . \qquad (105)$$

Inserting Ω_N into the phase characteristic above gives

$$\angle A_N = -N \tan^{-1}\left(\Omega_N \sqrt{\frac{\log 2}{N}} \right) = -\frac{\sqrt{N}}{1.20} \left\{ \Omega_N - \frac{.231}{N}\Omega_N^3 + \frac{.096}{N^2}\Omega_N^5 + \dots \right\} . \qquad (106)$$

As N raises, the nonlinear third, fifth, and higher order terms loose significance compared to the linear term. With more stages, the phase characteristic in the 3dB bandwidth $|\Omega_N|<1$ becomes more linear or - equivalently - the group delay stays more constant. The corresponding amplitude characteristic approaches a Gaussian curve in the passband. To see this we rewrite the amplitude expression using the fact that, cf.[8] p.228,

$$\lim_{x \to \infty} \left(1 + \frac{1}{x} \right)^x = e \quad \Rightarrow \quad \lim_{\Omega^2 \to 0} \left(1 + \Omega^2 \right)^{1/\Omega^2} = e \ . \qquad (107)$$

As bandwidth in measures of Ω reduces, the limit value is suited for large N, where we get

$$\left| \frac{A_N(j\Omega)}{A_{N0}} \right| = \left(1 + \Omega^2\right)^{-N/2} = \left[\left(1 + \Omega^2\right)^{1/\Omega^2} \right]^{\frac{-N\Omega^2}{2}} \underset{\Omega^2 \to 0}{\approx} e^{-\frac{N\Omega^2}{2}} = e^{-\frac{\log 2}{2}\Omega_N^2} . \quad (108)$$

The exponential gives a Gaussian characteristic due to the squaring of the frequency variable, and the last version shows readily that the scaling from Eq.(105) gives 3dB limits with $\Omega_N=\pm1$.

Butterworth Stagger Tuned Amplifiers

Each stage in a chain of amplifier stages provides a pole zero pattern corresponding to its load impedance. Synchronous tuning let the poles and zeros from all stages coincide. Staggering the pole-zero patterns gives provisions for a variety of amplification characteristics. We shall demonstrate the concept of stagger tuning by picking a simple but common case, the family of Butterworth characteristics of various order. They are defined by requiring maximal flatness in magnitude, which means that derivatives with respect to frequency up to the order 2N-1 are zero in the center at $\Omega=0$ [6]. The normalized N-th order Butterworth function is

$$\left| B_N(j\Omega) \right| \equiv \left| \frac{A_N(j\Omega)}{A_{N0}} \right| = \frac{1}{\sqrt{1 + \Omega^{2N}}} . \quad (109)$$

Examples of the magnitude characteristics are given in the upper part of Fig.37. The 3dB bandlimits corresponding to $\Omega=\pm1$ are independent of order, but as N increases the roll-off from the passband becomes more and more abrupt.

To find the pole patterns that give the normalized Butterworth characteristics, we start considering the squared magnitude,

$$\left| B_N(j\Omega) \right|^2 = \frac{1}{1 + \Omega^{2N}} . \quad (110)$$

Tracing back from $j\Omega$ along the imaginary axis to the corresponding normalized complex frequency variable S implies the substitutions

$$j\Omega = S \;\Rightarrow\; \Omega = -jS , \qquad \Omega^{2N} = (-1)^{2N} j^{2N} S^{2N} = (-1)^N S^{2N} , \quad (111)$$

$$\left| B_N(S) \right|^2 = \frac{1}{1 + (-1)^N S^{2N}} . \quad (112)$$

---

6) These and related concepts are part of the approximation problem in filter design. Consult ref´s [1], [2], or [3] for further details including the multitude of cases that are left out in this text.

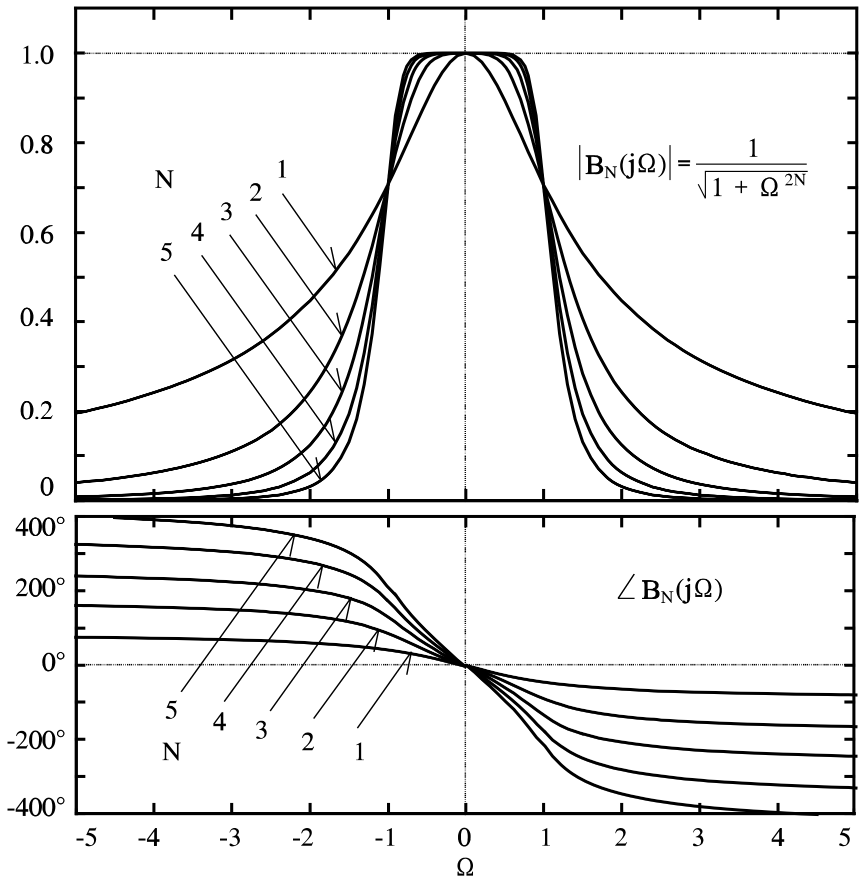

Fig.37 Normalized Butterworth characteristics of orders up to N=5. The phases are determined from pole positions like Fig.39.

Solving for the S values that set the denominator equal to zero provides poles for the squared magnitude

$$\textit{Poles of } \left|B_N\right|^2 : \quad 1 + (-1)^N S_p^{2N} = 0 \quad \Rightarrow \quad S_p^{2N} = (-1)^{N+1} = e^{j[(N+1)\pi + 2k\pi]} ,$$
$$S_p = e^{j\frac{\pi}{N}\left[\frac{N+1}{2} + k\right]} , \qquad k = 0, 1, \cdots, 2N-1 . \tag{113}$$

The poles are confined to the unit circle where they are equally spaced with an angle of π/N. When index k runs from 0 to 2N-1, all poles positions are covered once in the sequence sketched by Fig.38.

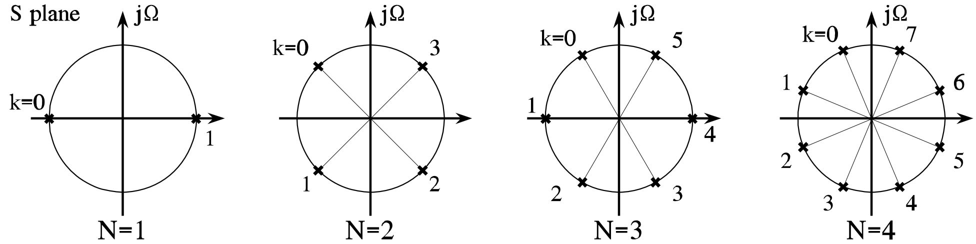

Fig.38 Pole patterns in N-th order Butterworth squared magnitude $|B_N(S)|^2$.

The Butterworth amplitude characteristic applies to lowpass as well as bandpass amplifiers. Both types may be realized using tuned LC circuits as interstage networks. The lowpass case ease the discussion because we transform from the normalized frequency Ω to the lowpass ω simply by multiplying with the bandwidth W_{3dB}. Thus, to represent a causal lowpass system, the basic requirements of having even real and odd imaginary parts along the imaginary frequency axis are met by imposing the condition

$$B_N^*(S) = B_N(-S) \quad \Rightarrow \quad B_N^*(j\Omega) = B_N(-j\Omega) \;, \tag{114}$$

so the squared amplitude function may be rewritten

$$\left| B_N(S) \right|^2 = B_N(S)\, B_N^*(S) = B_N(S)\, B_N(-S) \tag{115}$$

By the last factorization, poles of $|B_N|^2$ having positive real parts can be ascribed to $B_N(-S)$. This assures that the transfer function $B_N(S)$, which is targeted in circuit design, fulfills a necessary requirement of stability, as it only collects the N poles in the left half-plane. They were given by the first N indices in Eq.(113), in summary

$$\textit{Poles of } B_N(S) : \qquad S_{p,k} = e^{\,j\frac{\pi}{N}\left[\frac{N+1}{2}+k\right]} \,, \qquad k = 0,\, 1, \cdots, N-1 \;. \tag{116}$$

Pole positions in the second, third, and fourth order normalized Butterworth functions - also called prototype functions - are detailed in Fig.39.

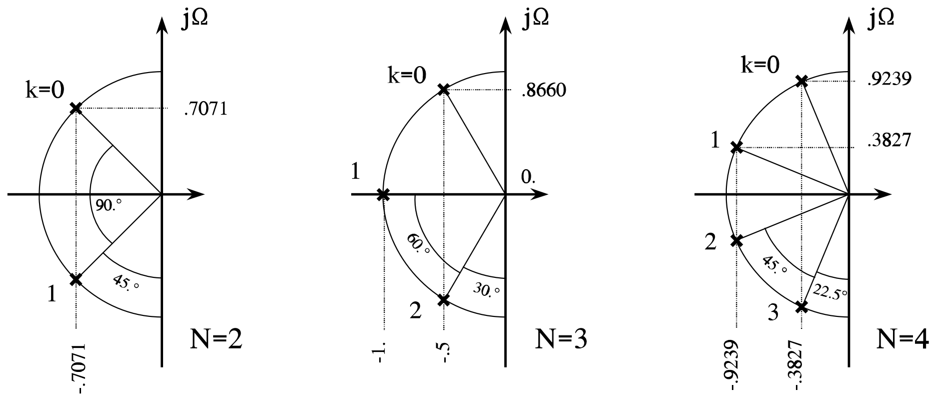

Fig.39 Examples of pole positions on the unit circle in normalized prototype Butterworth functions $B_N(S)$.

Poles $s_{p,k}$ in a bandpass amplifier of center frequency ω_0 and bandwidth W_{3dB} are related to the prototypes in Eq.(116) through the lowpass to bandpass transformation introduced in section II-3. Without any assumptions they provide

$$S_{p,k}\, W_{3dB} = s_{p,k} + \frac{\omega_0^2}{s_{p,k}} \qquad \Rightarrow \qquad s_{p,k} = \frac{S_{p,k}\, W_{3dB}}{2} \pm \sqrt{\left[\frac{S_{p,k}\, W_{3dB}}{2}\right]^2 - \omega_0^2} \;. \tag{117}$$

Under narrowband conditions, where $W_{3dB}/\omega_0 \ll 1$, the square root is dominated by its second term and the poles are approximated

$$narrowband\!: \quad \frac{W_{3dB}}{\omega_0} \ll 1 \quad \Rightarrow \quad s_{p,k} \quad \approx \quad \frac{S_{p,k}\; W_{3dB}}{2} \quad \pm \; j\,\omega_0 \; . \tag{118}$$

Thus, in narrowband we scale the prototype to half the desired bandwidth and copy the pole pattern from its lowpass center in origo to the bandpass centers at $s=\pm j\omega_0$. This process is demonstrated for a third order function in Fig.40.

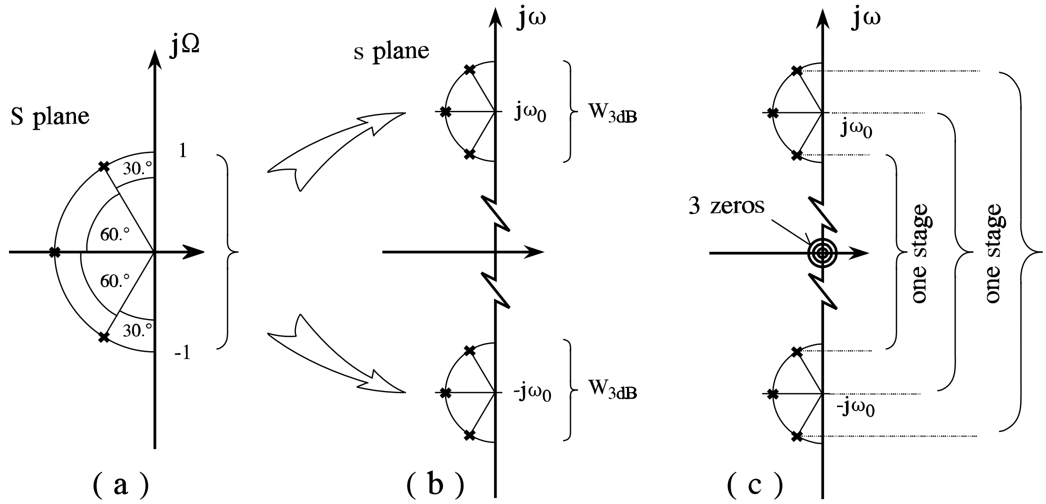

Fig.40 Mapping of Butterworth prototype poles (a) to poles in a narrowbanded bandpass amplifier (b). In (c) the poles are paired for stagger tuning that also requires three zeros in origo.

To realize the third order Butterworth characteristics exemplified by Fig.40(b), we need three basic parallel tuned stages. The idea of stagger tuning is to adjust the load of each stage to a required pole pair as indicated by Fig.40(c) and Fig.41. Fortunately, the parallel resonance circuits insert the necessary zeros at origo. As discussed in section II-3 they are not automatically encompassed by narrowband techniques. The sequence of pole pairs is arbitrary, but if we choose to let stage k realize the pole pair define by $s_{p,k}$ in Eq.(118), its resonance frequency ω_{0k} and quality factor Q_k are given by,

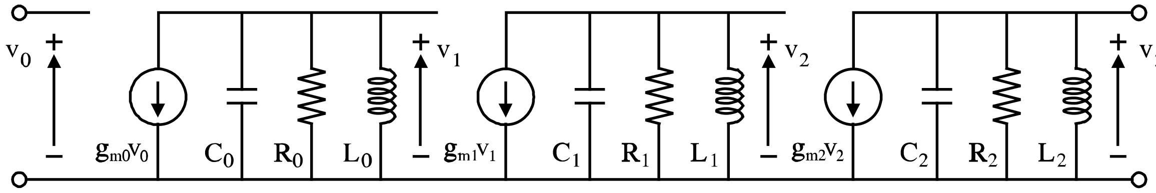

Fig.41 Three stage tuned amplifier. By stagger tuning the pole pair of each resonance circuit corresponds to at pole pair in the transfer function like the example in Fig.40(c).

$$s_{p,k} = -\frac{\omega_{0,k}}{2Q_k} \pm j\omega_{0,k} . \tag{119}$$

Pole positions determine the shape of the frequency response but not the absolute amplification level. The quantities ω_{0k},Q_k constrain the tuning components by

$$\omega_{0,k}^2 = 1/L_k C_k , \qquad Q_k = C_k \omega_{0,k} R_k . \tag{120}$$

It is a design decision to set the absolute impedance level. If the total amplifier is narrowbanded in the sense of $W_{3dB}/\omega_0 \ll 1$, each stage must be narrowbanded. By the approximation from Eq.(46) the gain of stage k, which realizes pole pair $s_{p,k}$ becomes

$$A_k(j\omega) = \frac{-g_{m,k}}{2C_k(j\omega - s_{p,k})} = \frac{-g_{m,k}}{2C_k\left(j\omega - j\omega_0 - \frac{1}{2} S_{p,k} W_{3dB}\right)} . \tag{121}$$

The last rewriting is based on Eq.(118) and refers back to the prototype function poles on the unit circle. At the center frequency $\omega=\omega_0$, stage k has the voltage gain

$$A_k(j\omega_0) = A_{k0} = \frac{g_{m,k}}{C_k W_{3dB} S_{p,k}} \quad\Rightarrow\quad |A_{k0}| = \frac{g_{m,k}}{C_k W_{3dB}} . \tag{122}$$

In a complete chain of stages for a Butterworth characteristic, there is a real, negative center frequency factor if the order is odd. The $S_{p,k}$'s in the remaining stages appear in complex conjugated pairs, so the center frequency gain of a N-th order stagger tuned Butterworth amplifier is given by

$$A_N(j\omega_0) = (-1)^N \frac{g_{m,0}\, g_{m,1} \cdots g_{m,N-1}}{C_0 C_1 \cdots C_{N-1} W_{3dB}^N} . \tag{123}$$

To elaborate further, the number of stages and an impedance strategy must be known. Consider as an example a third order amplifier where all transistor transconductances and load resistances are equal, $g_{m0}=g_{m1}=g_{m2}=g_m$ and $R_0=R_1=R_2=R_p$ respectively. We observe from the third order prototype in Fig.39 that the k=1 stage tunes to the center frequency. Using Eq.(119) we get

$$\frac{\omega_{0,1}}{2Q_1} = \frac{\omega_0}{2Q_1} = \frac{W_{3dB}}{2} \quad\Rightarrow\quad C_1 = \frac{Q_1}{R_p \omega_{0,1}} = \frac{1}{R_p W_{3dB}} . \tag{124}$$

The real values of poles with k=0 and k=2 are half the size of the k=1 pole, which gives

$$\frac{\omega_{0,0}}{2Q_0} = \frac{\omega_{0,2}}{2Q_2} = \frac{W_{3dB}}{4} \quad\Rightarrow\quad C_0 = C_2 = \frac{Q_0}{R_p \omega_{0,0}} = \frac{2}{R_p W_{3dB}} . \tag{125}$$

Knowing all capacitances, Eq.(123) provides the center frequency gain in this particular setup

$$A_3(j\omega_0) \;=\; -\,\frac{1}{4}\,\left[\,g_m\,R_p\,\right]^3. \tag{126}$$

To estimate gain-bandwidth factors if loading capacitances differ among the stages, the one with the smallest capacitance, i.e. the greatest single-stage GW, is commonly chosen as the reference. In the present amplifier this is clearly the C_1 stage, so we get

$$GBF \;=\; \frac{\sqrt[3]{\frac{1}{4}\,g_m\,R_p\,W_{3dB}}}{g_m/\,C_1} \;=\; \sqrt[3]{\frac{1}{4}} \;=\; 0.627\ . \tag{127}$$

Example II-5-2 (Butterworth amplifier)

By this example we change the components of the synchronously tuned amplifier from Example II-5-1. Keeping bandwidth, center frequency, and impedance level specifications, the frequency characteristic should now be of 2nd order Butterworth type. The task is to get the new component values and calculate the center frequency gain.

First we find the required pole-positions. Assuming narrowband condition we consider the pattern in the upper half-plane, Fig.42, where simple geometrical reflections give the coordinates of the poles.

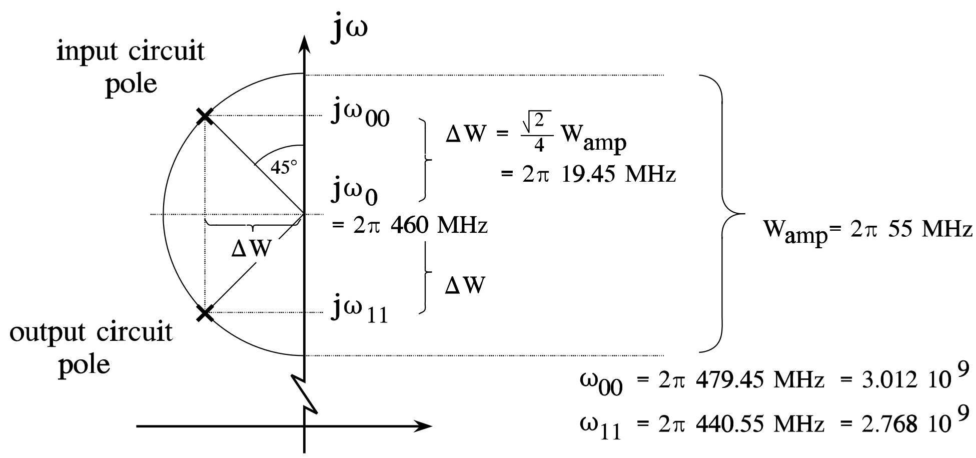

Fig.42

Associating the upper pole with the input circuit, the Q-factors of both tuned circuit are

$$Q_{00} = \frac{\omega_{00}}{2\,\Delta W} = \frac{479.45MHz}{2\cdot 19.45MHz} = 12.33, \qquad Q_{11} = \frac{\omega_{11}}{2\,\Delta W} = \frac{440.55MHz}{2\cdot 19.45MHz} = 11.33. \tag{128}$$

Using resistance figures from Example II-5-1, the tuning components now become

$$C_{00} = \frac{Q_{00}}{\omega_{00} R_{00}} = \frac{12.33}{3.012\,10^9 \cdot 65.55} = 62.42\,pF, \qquad C_0 = C_{00} - C_{in} = 62.42 - 6.5 = \underline{55.9\ pF},$$
$$L_0 = \frac{1}{\omega_{00}^2 C_{00}} = \frac{1}{3.012^2\,10^{18}\,62.39\,10^{-12}} = \underline{1.76\ nH}\ , \tag{129}$$

$$C_{11} = \frac{Q_{11}}{\omega_{11} R_{11}} = \frac{11.33}{2.768\,10^9 \cdot 74.55} = 54.88\,pF, \qquad C_1 = C_{11} - C_{out} = 54.88 - 1.6 = \underline{53.3\ pF},$$
$$L_1 = \frac{1}{\omega_{11}^2 C_{11}} = \frac{1}{2.768^2\,10^{18}\,54.94\,10^{-12}} = \underline{2.38\ nH}\ . \tag{130}$$

Recalling the discussion in the previous example, we are very close to practical bound on small inductances. Note, however, that Example II-6-4 shows one way to transform so component values stay practical. To find the center frequency gain Eq.(123) is used directly,

$$A_0 = \frac{(-1/R_g)\,g_m}{C_{00} C_{11} W_{amp}^2} = \frac{-\,0.2}{75.\cdot 62.39\cdot 10^{-12}\cdot 54.94\cdot 10^{-12}(2\,\pi\,55\cdot 10^6)^2} = \underline{-6.51} \sim 16.3dB\ . \tag{131}$$

Compared to synchronous tuning, Eq.(103), maximal flatness halves the voltage gain.

The synchronously tuned amplifier from Example II-5-1 is shown with the present stagger tuned Butterworth amplifier in Fig.43. The curves are simulated results from the equivalent

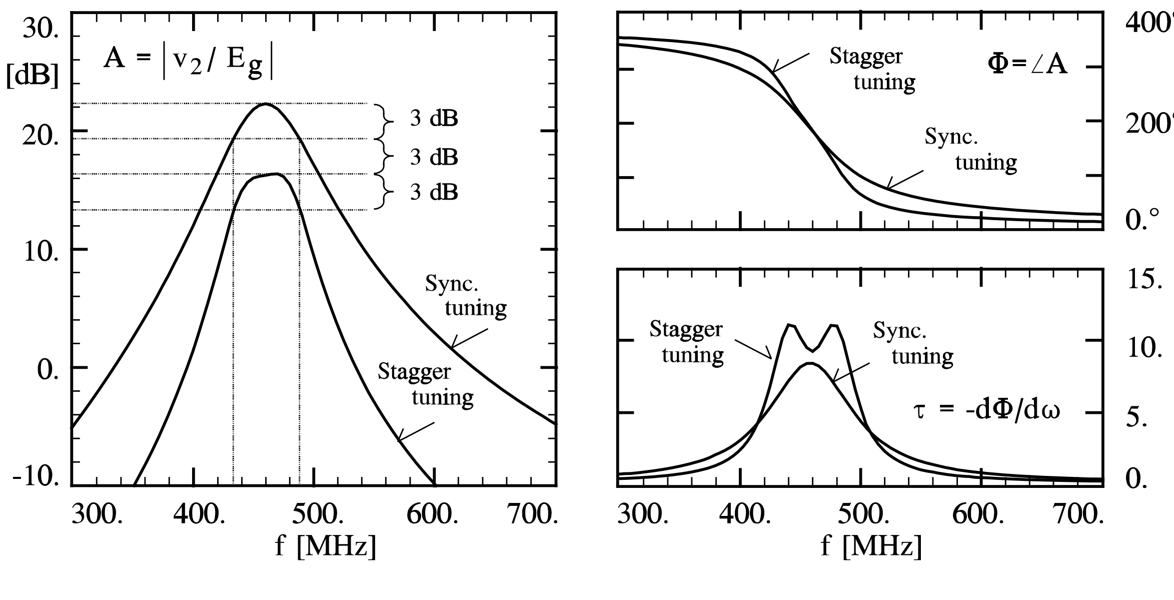

Fig.43 Simulated voltage gain magnitude, phase, and group delay for the synchronously and stagger tuned amplifiers in Examples II-5-1 and 2. Narrowband approximated circuit data are used.

circuit in Fig.36 without further assumptions. It is therefore worth noticing how close we come to the specifications regarding gain and bandlimits, although all underlying component calculations were based on narrowband assumptions. The most visible consequence of the simplifications is the lack of complete flatness in stagger tuning. Had the poles been correctly found by solving Eq.(117) instead of the simpler scaling and copying approach in Eq.(118), the result improves as will be seen below. From a design point of view it is dubious to go further analytically. Practical component values need fine-tuning, either physically or by circuit optimization, to compensate other design simplifications, for instance the employment of uncomplicated transistor models or the ignorance of parasitic elements in the lay-out. The simple narrowband methods give a good starting point for this process. However, in the present context we shall enlighten the assumptions and approximations behind narrowband methods whenever possible and therefore compare the previous result with their true counter-parts. Applying prototype poles to Eq.(117) gives

$$S_{p0,1} = \frac{1}{\sqrt{2}}\,(-1 \pm j) \quad , \quad \omega_0 = 2\pi \cdot 460\,MHz \quad \Rightarrow$$
$$\left\{ \begin{array}{l} s_{p0} = \dfrac{-\omega_{00}}{2Q_{00}} \pm j\omega_{00} = 2\pi\,\{-20.267\cdot 10^6 \pm j\,479.45\cdot 10^6\} \Rightarrow Q_{00} = 11.827 \\ s_{p1} = \dfrac{-\omega_{11}}{2Q_{11}} \pm j\omega_{11} = 2\pi\,\{-18.623\cdot 10^6 \pm j\,440.55\cdot 10^6\} \Rightarrow Q_{11} = 11.828 \end{array} \right. \tag{132}$$

Realize that by this calculation we give up the narrowband assumptions in the complete Butterworth amplifier characteristics. To identify Q_{00},ω_{00} or Q_{11},ω_{11} from the pole positions, narrowband assumptions about the individual stages are maintained. With Q-factors over 10, Eq.(43) shows, that this is still a very satisfactory assumption. Having established the Q-factor and resonance frequencies for the two stages, computations similar to Eqs.(129), (130) lead to new components values,

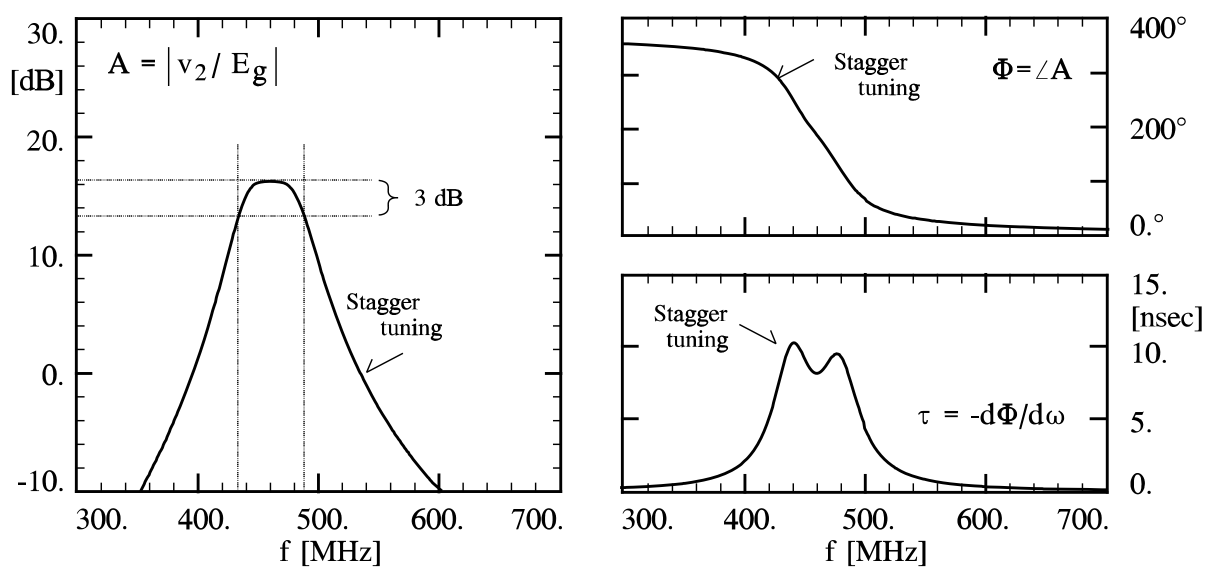

Fig.44 Simulated voltage gain magnitude, phase, and group delay for stagger tuned amplifier in Examples II-5-2. True pole positions are used to calculate circuit data.

$$C_0 = 53.4pF, \qquad L_0 = 1.84nH, \qquad C_1 = 57.7pF, \qquad L_1 = 2.28nH. \tag{133}$$

Fig.44 shows the simulated frequency response obtained by these data, and clearly the flatness in magnitude has improved. The reason why group delay no longer gets symmetric appearance is the fact, that the Butterworth characteristic is symmetric in the normalized frequency Ω, not in ω with respect to which, the phase was differentiated.

Example II-5-2 end

II-6 Transformers and Transformerlike Couplings

Needs for transforming signal and impedance levels in RF circuits are both frequent and diversified, so a multitude of approaches and techniques are available for solving that sort of problems. Among them are the conventional magnetically coupled transformer, which is a highly useful component at frequencies up to approximately 3 GHz. We shall consider transformers and circuits that behave similarly in some depth in this section. The scopes are to gain basic understanding of advantages and limitations of transformer couplings, and to provide a background for setting up simulator models. Some simulation programs are sparsely equipped with the coupled inductor and transformer models that are needed in RF-design, so they must be build from basic circuit functions and components.

Review of Mutual Inductances

Two or more inductors have mutual inductance if they interact through their magnetic fields. To fix ideas we start considering two inductors where - as shown in Fig.45 - currents are separately applied. Superposition of the two conditions gives the following expressions for terminal voltages and the total magnetic fluxes Φ_1 and Φ_2 through the inductors,

$$\begin{bmatrix} v_1 \\ v_2 \end{bmatrix} = \begin{bmatrix} v_{11} + v_{12} \\ v_{21} + v_{22} \end{bmatrix} = \frac{d}{dt}\begin{bmatrix} \Phi_1 \\ \Phi_2 \end{bmatrix} = \frac{d}{dt}\begin{bmatrix} \Phi_{11} + \Phi_{12} \\ \Phi_{21} + \Phi_{22} \end{bmatrix} = \begin{bmatrix} L_1 \\ M_{21} \end{bmatrix}\frac{di_1}{dt} + \begin{bmatrix} M_{12} \\ L_2 \end{bmatrix}\frac{di_2}{dt} \,. \tag{134}$$

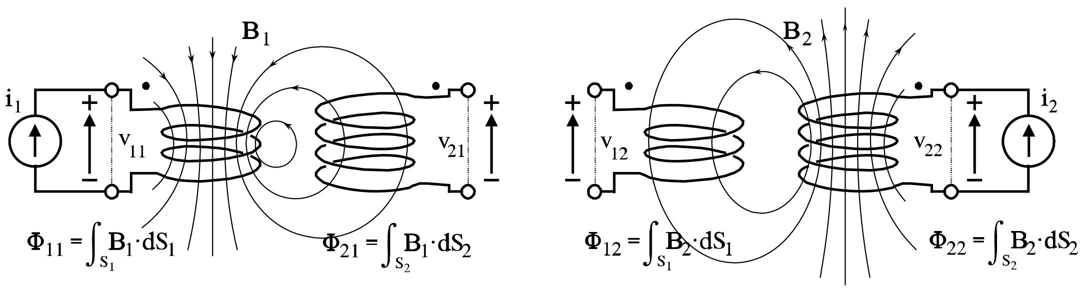

Fig.45 Inductors with mutual inductance. Surfaces for the flux integrals are bounded by the coils and lines through the terminals. Dots indicate orientation. Current entering a dotted terminal support flux in the other coil.

The flux integrals condense in the inductances L_1, L_2, and the mutual inductances M_{12}, M_{21}. They are factors of proportionality between inductor currents and the different flux contributions. The factors are the elements of an inductance matrix, which finally gives the two-port impedance matrix for two coupled inductors,

$$\begin{bmatrix} v_1(s) \\ v_2(s) \end{bmatrix} = s\begin{bmatrix} \Phi_1(s) \\ \Phi_2(s) \end{bmatrix} = s\begin{bmatrix} L_1 & M_{12} \\ M_{21} & L_2 \end{bmatrix}\begin{bmatrix} i_1(s) \\ i_2(s) \end{bmatrix} = \begin{bmatrix} z_{11}(s) & z_{12}(s) \\ z_{21}(s) & z_{22}(s) \end{bmatrix}\begin{bmatrix} i_1(s) \\ i_2(s) \end{bmatrix} \,. \tag{135}$$

Including more than two inductors, the equations are generalized to

$$\boldsymbol{v}(s) = s\,\boldsymbol{\Phi}(s) = s\,\boldsymbol{L}\,\boldsymbol{i}(s) = \boldsymbol{Z}(s)\,\boldsymbol{i}(s)\,. \tag{136}$$

Here **v**, **Φ**, and **i** are vectors holding the port voltages, fluxes, and currents respectively, while **L** and **Z** are the inductance and impedance matrices. The inductance matrix is assumed to be symmetric and positive definite or semidefinite. The first property expresses reciprocity, which apply if the inductors have isotropic surroundings. It evolves from the renowned Lorentz reciprocity theorem, [4] sec.2.12,4.5 , and causes the total magnetic energy to depend only upon the instant current vector, no matter how it behaved in the past. The second property is a passivity requirement ensuring that starting from zero initial conditions, the total stored magnetic energy will always be positive or zero, [9] chap.15. In mathematical terms, the requirements are that all subdeterminants of **L**, which can be taken symmetrically around the diagonal, must be positive or zero, cf.[10] sec.7.2.

With two coupled inductors, the reciprocity and passivity conditions become

$$\textit{Reciprocity}:\quad M \equiv M_{12} = M_{21}\,, \quad \Rightarrow \quad z_{12}(s) = z_{21}(s)\,, \tag{137}$$

$$\textit{Passivity}:\quad L_1 \geq 0, \quad L_2 \geq 0, \quad L_1 L_2 - M^2 \geq 0 \;\Rightarrow\; |M| \leq \sqrt{L_1 L_2}\,. \tag{138}$$

The limit cases of L_1=0 or L_2=0 implying M=0 are of no practical interest. Mutual inductances are often expressed by the coupling coefficient k,

$$k \equiv M / \sqrt{L_1 L_2}\,, \qquad \textit{where} \quad -1 \leq k \leq 1\,. \tag{139}$$

In circuit schematics, mutual inductances may be represented as shown in Fig.46(a,b). If we start fixing the orientations of the two ports, the sign of M and k is implicitly determined. Applying a positive current to port one, M and k are positive if both port voltages are in phase, negative if they are 180° out of phase. To emphasize phases rather than the more arbitrary port orientation, the dot-convention, which defined flux directions in Fig.45, will also tag a set of terminals that gives in-phase port voltages. Using port orientations opposite the dot indication implies negative mutual inductances or couplings as shown in the figure.

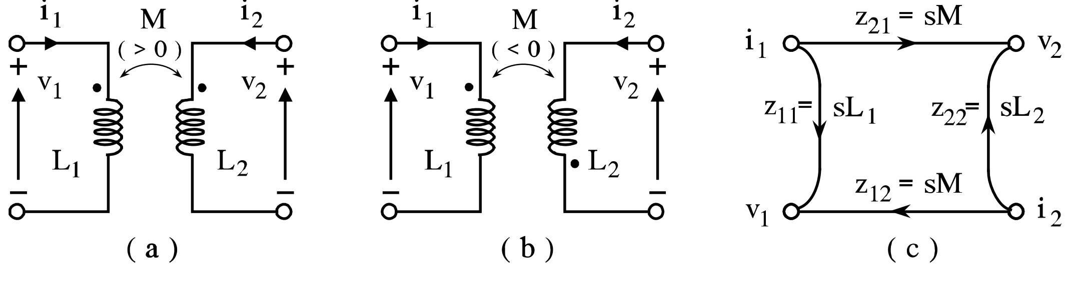

Fig.46 Inductors with (a) positive and (b) negative mutual inductances following the dot-convention from Fig.45. The signal flow-graph represents the z-parameter matrix.

The borderline to passivity, |k|=1, is called tight or close coupling and is one goal aimed upon when mutual inductances are employed in transformers. With k=±1 the two voltage equations that stem from Eq.(135) become

$$\begin{aligned} v_1 &= \quad sL_1\, i_1 \quad \pm s\sqrt{L_1 L_2}\, i_2 \\ v_2 &= \pm s\sqrt{L_1 L_2}\, i_1 \quad + sL_2\, i_2 \end{aligned} \tag{140}$$

However, the inductance matrix is singular in this case, so the two equations are linearly related, and the lower equation follows from the upper one

$$\pm\sqrt{\frac{L_2}{L_1}}\, v_1 = \pm\, s\,\sqrt{L_1 L_2}\, i_1 \;+\; s\, L_2\, i_2 = v_2 \ . \tag{141}$$

The square root of the inductance ratio is called the winding or turns ratio N, because the inductances of typical transformer coils are proportional to the squared number of windings, cf.[7] sec.4.8. Equation (141) expresses the transformer voltage relationship

$$v_2 = N\, v_1 \ , \qquad N\,\Big|_{|k|=1} = \pm\sqrt{\frac{L_2}{L_1}} \ . \tag{142}$$

To share and confine the magnetic field, the inductances are often wound on a core of high permeability material, for instance a toroide like Fig.47. The phrases of tight or close couplings refer to the fact, that the two inductors must encompass the same magnetic flux when |k|=1. Suppose the two coils are similar so they have the same ratio A_L between inductance and the squared winding count,

$$L_1 = A_L N_1^2 \ , \qquad \textit{and} \qquad L_2 = A_L N_2^2 \ .$$

With k=±1, the flux per winding in L_2 that originates from current i_1 equals in size the flux per winding in L_1,

$$\frac{\Phi_{21}}{N_2} = \frac{M\, i_1}{N_2} = \frac{\pm\sqrt{L_1 L_2}\, i_1}{\sqrt{L_2 / A_L}} = \pm\sqrt{A_L L_1}\, i_1 = \pm\frac{L_1 i_1}{N_1} = \pm\frac{\Phi_{11}}{N_1} \ . \tag{144}$$

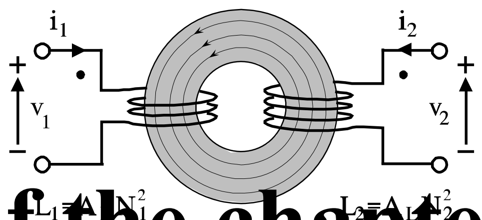

Fig.47 Toroidal transformer where both inductors share the same magnetic field.